



## The first iron(III) complexes with cyclin-dependent kinase inhibitors: Magnetic, spectroscopic (IR, ES+ MS, NMR, $^{57}\text{Fe}$ Mössbauer), theoretical, and biological activity studies

Zdeněk Trávníček<sup>a,\*</sup>, Igor Popa<sup>a</sup>, Michal Čajan<sup>a</sup>, Radek Zbořil<sup>b</sup>, Vladimír Kryštof<sup>c</sup>, Jiří Mikulík<sup>a</sup>

<sup>a</sup> Department of Inorganic Chemistry, Faculty of Science, Palacký University, Tř. 17. listopadu 12, CZ-779 00, Olomouc, Czech Republic

<sup>b</sup> Department of Physical Chemistry and Nanomaterials Research Centre, Faculty of Science, Palacký University, Tř. 17. listopadu 12, CZ-779 00, Olomouc, Czech Republic

<sup>c</sup> Laboratory of Growth Regulators, Faculty of Science, Palacký University, Štechtitelů 11, CZ-783 71, Olomouc, Czech Republic

### ARTICLE INFO

#### Article history:

Received 1 July 2009

Received in revised form 23 November 2009

Accepted 30 November 2009

Available online 5 December 2009

#### Keywords:

Iron(III) complexes

$^{57}\text{Fe}$  Mössbauer spectroscopy

CDK inhibition

*In vitro* cytotoxicity

DFT calculations

### ABSTRACT

The first  $\text{Fe}^{\text{III}}$  complexes **1–6** with cyclin-dependent kinase (CDK) inhibitors of the type  $[\text{Fe}(\text{L}_n)\text{Cl}_3] \cdot n\text{H}_2\text{O}$  ( $n = 0$  for **1**, 1 for **2**, 2 for **3–6**;  $\text{L}_1\text{–L}_6 = \text{C}2\text{-}$  and phenyl-substituted CDK inhibitors derived from 6-benzylamino-9-isopropylpurine), have been synthesized and characterized by elemental analysis, IR,  $^{57}\text{Fe}$  Mössbauer,  $^1\text{H}$  and  $^{13}\text{C}$  NMR, and ES+ mass spectroscopies, conductivity and magnetic susceptibility measurements, and thermogravimetric analysis (TGA) and differential scanning calorimetry (DSC). The study revealed that the compounds are mononuclear, tetrahedral high-spin ( $S = 5/2$ )  $\text{Fe}^{\text{III}}$  complexes with an admixture of an  $S = 3/2$  spin state originating probably from five-coordinated  $\text{Fe}^{\text{III}}$  ions either connecting with a bidentate coordination mode of the CDK inhibitor ligand or relating to the possibility that one crystal water molecule enters the coordination sphere of the central atom in a portion of molecules of the appropriate complex. Nearly spin-only value of the effective magnetic moment ( $5.82 \mu_{\text{eff}}/\mu_{\text{B}}$ ) was determined for compound **1** due to absence of crystal water molecule(s) in the structure of the complex. Based on NMR data and DFT calculations, we assume that the appropriate organic ligand is coordinated to the  $\text{Fe}^{\text{III}}$  ion through the N7 atom of a purine moiety. The cytotoxicity of the complexes was tested *in vitro* against selected human cancer cell lines (*G-361*, *HOS*, *K-562* and *MCF-7*) along with the ability to inhibit the CDK2/cyclinE kinase. The best cytotoxicity ( $\text{IC}_{50}$ : 4–23  $\mu\text{M}$ ) and inhibition activity ( $\text{IC}_{50}$ : 0.02–0.09  $\mu\text{M}$ ) results have been achieved in the case of complexes **2–4**, and complexes **3**, **4** and **6**, respectively. In addition, the X-ray structure of 2-chloro-6-benzylamino-9-isopropylpurine, i.e. a precursor for the preparation of **L1**, **L4** and **L5**, is also described.

© 2009 Elsevier Inc. All rights reserved.

### 1. Introduction

Protein kinases are enzymes that catalyze phosphorylation of suitable protein substrates, which in turn change their conformation and more importantly also their activity. Timely and spatially controlled protein kinases therefore participate nearly in all aspect of cell biology [1]. However, recently published works proved that mutations and dysregulations of protein kinases should lead to initiation of many human diseases. Cyclin-dependent kinases (CDKs) form a subgroup of serine/threonine protein kinases controlling many cellular events, including a cell cycle division [2]. CDKs are frequently deregulated in cancer cells, so these enzymes represent rational drug targets [3]. To date, many pharmacological inhibitors of CDKs have been identified and the most active of them already undergo clinical trials as new anticancer drugs [4,5]. One of them,

*R-roscovitine* is one of the first selective inhibitors of CDKs, identified through structure–activity relationships study of 2,6,9-trisubstituted purines [6,7]. As demonstrated by X-ray crystallography, it binds specifically to the active site of CDK2 and thus interferes with its catalytic function [8]. Moreover, *R-roscovitine* inhibits also CDK9 that phosphorylates and thus activates C-terminus of RNA polymerase II. Its inhibition triggers insufficient transcription of many genes, especially those with short half-lived mRNAs and proteins like oncogenic Hdm2, D and B cyclins, or anti-apoptotic Mcl-1 [9,10], which leads to cell cycle arrest and/or apoptosis of cancer cells. The one of the most recent works even suggests that CDK9 inhibitors of transcription could also serve as potential drugs against tumour invasion and metastasis [11]. In July 2006, the chiral form (*R*) of *roscovitine* entered a Phase IIb of the clinical trials under code names of *CYC202* and *seliciclib* (Cyclacel Pharmaceuticals, Inc., [www.cyclacel.com](http://www.cyclacel.com)). Hitherto, some of 2,6,9-trisubstituted purines, that are N6-modified by the above described manner, were used as ligands for the preparation of the cytotoxic

\* Corresponding author. Tel.: +420 585 634 944; fax: +420 585 634 954.

E-mail address: [zdenek.travnicek@upol.cz](mailto:zdenek.travnicek@upol.cz) (Z. Trávníček).

transition metal complexes [e.g. Pt<sup>II</sup>, Pd<sup>II</sup>, Cu<sup>II</sup>, Zn<sup>II</sup>] in our previous papers [12–14].

Recently, we have published two papers regarding the synthesis and characterization of Fe<sup>II</sup> and Fe<sup>III</sup> complexes involving 2,6,9-tri-substituted purines. The first of them describes the preparation of the (H<sup>+</sup>L)<sub>2</sub>[FeCl<sub>3</sub>] ionic pair compound [15], where H<sup>+</sup>L stands for a protonated form of *bohémine*, i.e. 2-[(3-hydroxypropyl)amino]-6-benzylamino-9-isopropylpurine, while the second one [16] deals with the study of complexes having the composition of [Fe(L)Cl<sub>3</sub>] $\cdot$ H<sub>2</sub>O, where ligands L are N6-benzyladenosine derivatives with variously modified benzyl rings. Moreover, there are only a few works in the literature describing the preparation and study of Fe<sup>II,III</sup> complexes with some adenine or purine derivatives. For instance, Fe<sup>III</sup> complexes with non-substituted adenine (adH), e.g. {[Cl(H<sub>2</sub>O)(ad)Fe- $\mu$ -(adH)-Fe(H<sub>2</sub>O)Cl<sub>2</sub>]<sub>n</sub> [17], [Fe(adH)<sub>2</sub>Cl<sub>3</sub>] [18], [(ClO<sub>4</sub>)(adH)<sub>2</sub>Fe- $\mu$ -(adH)<sub>2</sub>-Fe(adH)<sub>2</sub>(ClO<sub>4</sub>)](ClO<sub>4</sub>)<sub>4</sub> and [Fe(ad)(ClO<sub>4</sub>)] $\cdot$ EtOH $\cdot$ 2H<sub>2</sub>O [19]], were reported. However, all of these complexes have been characterized by elemental analyses, room temperature magnetochemical, spectroscopic (UV–VIS, IR) and conductometric measurements, and their potential biological activity was not ever tested. With respect to Fe-complexes containing purine skeleton in their structure, only three X-ray structures [20,21] were determined and deposited within the Cambridge Crystallographic Data Centre up to now, namely [Fe<sup>II</sup>(5-imp)(H<sub>2</sub>O)<sub>5</sub>] $\cdot$ 2H<sub>2</sub>O (5-imp = inosine-5-monophosphate) [20], [Fe<sup>II</sup>(5-gmp)(H<sub>2</sub>O)<sub>5</sub>] $\cdot$ 3H<sub>2</sub>O (5-gmp = guanosine-5-monophosphate) [21] and [Fe<sup>II</sup>(6-mp)<sub>3</sub>Fe<sup>III</sup>Cl<sub>4</sub>]Cl (6-mp = 6-mercaptapurine) [21].

Together with all other results, we also bring here a detailed interpretation of <sup>57</sup>Fe Mössbauer spectra, which showed the diversity of geometric arrangements in the vicinity of the central Fe atoms in the prepared compounds, and which is interrelated with

electronic structure of Fe<sup>III</sup> ions. Besides, the goal of this study was to prepare Fe<sup>III</sup> complexes showing significant *in vitro* cytotoxicity against some human cancer cell lines and thus, to obtain compounds having possibility to find the utilization as drug candidates in anticancer therapy.

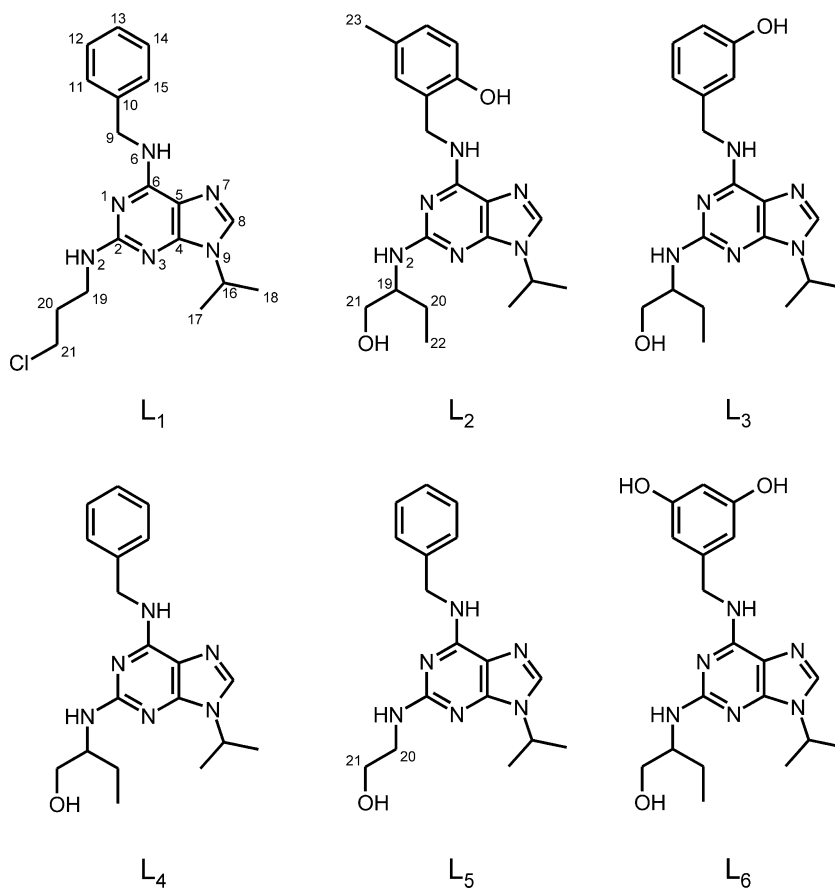
## 2. Results and discussion

### 2.1. Chemistry and general features

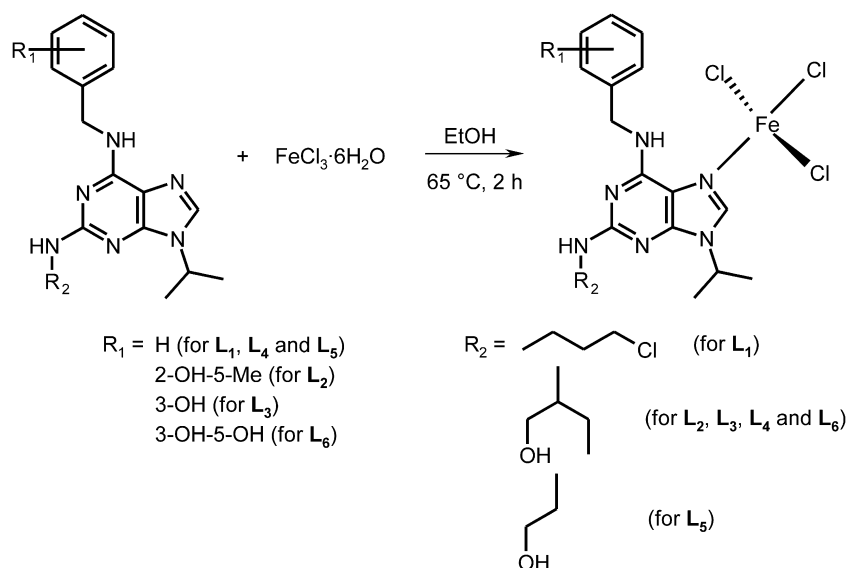
The reaction of FeCl<sub>3</sub> $\cdot$ 6H<sub>2</sub>O with the corresponding CDK inhibitor, L<sub>n</sub> (see Schemes 1 and 2) in an ethanolic solution in a molar ratio 1:1 led to formation of mononuclear complexes of [Fe(L<sub>n</sub>)Cl<sub>3</sub>] $\cdot$ xH<sub>2</sub>O (x = 0 for **1**, x = 1 for **2**, and x = 2 for **3–6**). The prepared compounds are hygroscopic (they need to be stored in desiccator over P<sub>4</sub>O<sub>10</sub> as a drying medium), well soluble in ethanol, acetone, *N,N'*-dimethylformamide (DMF), dimethyl sulfoxide (DMSO), partially soluble in water, and insoluble in diethylether. Their colours, analytical data, effective magnetic moment values and molar conductivities are listed in Table 1, while the most important infrared spectral data are summarized in Table 2. The molar conductivity values (1.1–5.4 S cm<sup>2</sup> mol<sup>-1</sup> in methanol and 4.1–16.8 S cm<sup>2</sup> mol<sup>-1</sup> in acetone) clearly showed the non-ionic feature of the studied complexes **1–6** in the solvents used [22]. No change in conductivity values was achieved after 24 h.

### 2.2. <sup>57</sup>Fe Mössbauer spectroscopy and magnetochemistry

Hyperfine parameters of room temperature Mössbauer spectra are summarized in Table 3. As can be clearly seen from the table,



**Scheme 1.** A representation of 6-benzylamino-9-isopropylpurine derivatives, L<sub>1</sub>–L<sub>6</sub>, used as organic ligands for the preparation of the Fe<sup>III</sup> complexes (**1–6**).



**Scheme 2.** A general pathway for the synthesis of the  $\text{Fe}^{\text{III}}$  complexes **1–6**.

**Table 1**

Colour, magnetic and molar conductivity data of the complexes **1–6**.

Compound	Colour	$\mu_{\text{eff}}/\mu_{\text{B}}$	$\lambda_{\text{M}}$ ( $\text{S cm}^2 \text{ mol}^{-1}$ )	
			a	b
$[\text{Fe}(\mathbf{L}_1)\text{Cl}_3]$ ( <b>1</b> )	Brownish red	5.82	5.4	16.8
$[\text{Fe}(\mathbf{L}_2)\text{Cl}_3]\cdot\text{H}_2\text{O}$ ( <b>2</b> )	Brown	5.20	2.5	4.4
$[\text{Fe}(\mathbf{L}_3)\text{Cl}_3]\cdot 2\text{H}_2\text{O}$ ( <b>3</b> )	Brownish orange	5.21	1.2	4.6
$[\text{Fe}(\mathbf{L}_4)\text{Cl}_3]\cdot 2\text{H}_2\text{O}$ ( <b>4</b> )	Brownish orange	5.00	1.1	5.1
$[\text{Fe}(\mathbf{L}_5)\text{Cl}_3]\cdot 2\text{H}_2\text{O}$ ( <b>5</b> )	Brownish orange	5.33	1.5	12.0
$[\text{Fe}(\mathbf{L}_6)\text{Cl}_3]\cdot 2\text{H}_2\text{O}$ ( <b>6</b> )	Brown	5.24	3.1	4.1

<sup>a</sup> Measured in methanol.

<sup>b</sup> Measured in acetone.

Mössbauer spectra of complexes **2–6** are very similar with two spectral components differing mainly in quadrupole splitting parameters, while the isomer shift parameters lie in the narrow range of  $0.32\text{--}0.35 \text{ mm s}^{-1}$ . The presence of two fitted subspectra may be associated with the existence of two non-equivalent structural and spin states of iron within the compounds, although the values of isomer shift clearly indicate the formal oxidation state of  $3+$ . The minor component with the spectral area, varying between 20% and 25%, shows a relatively higher quadrupole split-

ting ( $\Delta E_Q = 0.96\text{--}1.02 \text{ mm s}^{-1}$ ), which may be connected with decreasing the symmetry in the vicinity of the central atoms as compared to the major component. Thus, it may be concluded that the above-mentioned  $\Delta E_Q$  values may be ascribed to a trigonal-bipyramidal coordination with the  $3/2$  spin state of iron, where either one crystal water molecule is probably coordinated to iron or the corresponding  $L_n$  ligand is coordinated as a bidentate one. The major (70–75% of spectrum area) component reveals a relatively low quadrupole splitting ( $\Delta E_Q = 0.56\text{--}0.58 \text{ mm s}^{-1}$ ) which may be ascribed to a distorted tetrahedral geometry. To distinguish between two probable structural types, the Mössbauer spectrum of representative sample (compound **4**) was measured at 5 K (Fig. 1). As a result, the sextet ( $\delta = 0.57 \text{ mm s}^{-1}$ ) corresponding to the presence of  $\text{Fe}^{\text{III}}$  species probably with the coordination number of 5 was observed in the spectrum together with the singlet having the isomer shift of  $0.41 \text{ mm s}^{-1}$ . This value is characteristic for tetrahedrally coordinated  $\text{Fe}^{\text{III}}$  ions [23] and even lower than expected due to the temperature decreasing. It seems that the higher values of isomer shifts in room temperature spectra corresponding to tetrahedral  $\text{Fe}^{\text{III}}$  ( $\delta = 0.32\text{--}0.35 \text{ mm s}^{-1}$ ) cations are caused by the presence of water molecules in an outer coordination sphere, while this effect is suppressed at low temperatures.

**Table 2**

Selected IR spectral data ( $\text{cm}^{-1}$ ) of the complexes **1–6**.

Compound	$\nu(\text{C}=\text{N})$	$\nu(\text{C}=\text{C})$	$\nu(\text{C}_{\text{ar}}-\text{O})$	$\nu(\text{C}_{\text{alif}}-\text{O})$	$\nu(\text{Fe}-\text{Cl})$	$\nu(\text{Fe}-\text{N})$
$[\text{Fe}(\mathbf{L}_1)\text{Cl}_3]$ ( <b>1</b> )	1638s	1581m 1452m	–	–	381s	333w
$[\text{Fe}(\mathbf{L}_2)\text{Cl}_3]\cdot\text{H}_2\text{O}$ ( <b>2</b> )	1635s	1572m 1461m	1214m	1049m	384s	328w
$[\text{Fe}(\mathbf{L}_3)\text{Cl}_3]\cdot 2\text{H}_2\text{O}$ ( <b>3</b> )	1637s	1589s 1459m	1215m	1051m	381s	332w
$[\text{Fe}(\mathbf{L}_4)\text{Cl}_3]\cdot 2\text{H}_2\text{O}$ ( <b>4</b> )	1634s	1571m 1453m	–	1051m	382s	330w
$[\text{Fe}(\mathbf{L}_5)\text{Cl}_3]\cdot 2\text{H}_2\text{O}$ ( <b>5</b> )	1635s	1574s 1453m	–	1060m	381s	330w
$[\text{Fe}(\mathbf{L}_6)\text{Cl}_3]\cdot 2\text{H}_2\text{O}$ ( <b>6</b> )	1638s	1576m 1459m	1214m	1049m	382s	331w
$[\text{Fe}(\mathbf{L}_1)\text{Cl}_3]$ ( <b>1a</b> ) <sup>a</sup>	1642s	1627s 1535m 1489m	–	–	403m 411m	344w

<sup>a</sup> The values belonging to the optimized structure **1a** (see Fig. 4a) and calculated by B3LYP/6–311G\*/Wachter's level.

**Table 3**  
<sup>57</sup>Fe Mössbauer spectral parameters of the complexes **1–6**.

Compound	Component	T (K)	$\delta \pm 0.01$ (mm s <sup>-1</sup> )	$\Delta E_Q \pm 0.01$ (mm s <sup>-1</sup> )	$\Gamma \pm 0.01$ (mm s <sup>-1</sup> )	RA $\pm 1$ (%)
<b>1</b>	Doublet	300	0.25	0.30	0.40	100
	Singlet	5	0.40	–	–	100
<b>2</b>	Doublet	300	0.34	0.57	0.39	80
	Doublet	300	0.33	0.99	0.30	20
<b>3</b>	Doublet	300	0.35	0.56	0.34	79
	Doublet	300	0.33	0.99	0.37	21
<b>4</b>	Doublet	300	0.35	0.56	0.38	76
	Doublet	300	0.34	0.96	0.33	24
	Singlet	5	0.41	–	–	46
	Sextet	5	0.57	-0.18 <sup>a</sup>	46.7 <sup>b</sup>	54
<b>5</b>	Doublet	300	0.35	0.35	0.35	75
	Doublet	300	0.34	0.97	0.30	24
<b>6</b>	Doublet	300	0.34	0.58	0.37	79
	Doublet	300	0.32	1.02	0.30	20
<b>1a</b> <sup>c</sup>	Doublet	0	0.364			
<b>1b</b> <sup>c</sup>	Doublet	0	0.384			
<b>1c</b> <sup>c</sup>	Doublet	0	0.478			
<b>1d</b> <sup>c</sup>	Doublet	0	0.450			

$\delta$  – Isomer shift related to metallic iron,  $\Delta E_Q$  – quadrupole splitting,  $\Gamma$  – full width at a half of maximum, RA – percentage of subspectrum area related to iron content.

<sup>a</sup>  $\varepsilon_Q$  – quadrupole shift (mm s<sup>-1</sup>).

<sup>b</sup>  $H$  – hyperfine magnetic field (T).

<sup>c</sup> Theoretically calculated values based on optimized geometries of the predicted molecular structures of the complex **1** (for structural details, see the Fig. 4 and Table 4). The calculations were performed at 0 K and vacuum, thus the value of the temperature Doppler shift (ca. 0.10–0.12 mm s<sup>-1</sup> for Fe-complexes) has to be applied to correct the corresponding values to the values at room temperature.

The interpretation of the room temperature <sup>57</sup>Fe Mössbauer spectrum of the anhydrous complex **1** is not as complicated as it consists of one doublet with the lower isomer shift ( $\delta = 0.25$  mm s<sup>-1</sup>) compared to complexes **2–6**, thus giving an evidence for tetrahedral Fe<sup>III</sup> compounds with an  $S = 5/2$ . This difference confirms the above-mentioned prediction of the important influence of the crystal water molecules on the hyperfine parameters [24]. The low temperature spectrum (5 K) of complex **1** yields the singlet with almost the same  $\delta$  parameter as in the case of the complex **4**, thus proving the suppression of the distortion caused by water molecule in the vicinity of the central atom.

The magnetic susceptibility of all complexes have been measured at room temperature, and the calculated values of effective magnetic moment  $\{\mu_{\text{eff}} = 2.828(\chi_M \cdot T)^{1/2} \cdot \mu_B\}$  are as follows: 5.82  $\mu_{\text{eff}}/\mu_B$  for compound **1**, 5.20  $\mu_{\text{eff}}/\mu_B$  for **2**, 5.21  $\mu_{\text{eff}}/\mu_B$  for **3**, 5.00  $\mu_{\text{eff}}/\mu_B$  for **4**, 5.33  $\mu_{\text{eff}}/\mu_B$  for **5**, and finally 5.24  $\mu_{\text{eff}}/\mu_B$  for **6** (see Table 1). Accordingly, the  $\chi_M \cdot T$  values are 4.235 cm<sup>3</sup> K mol<sup>-1</sup> (for **1**) and between 3.126 and 3.552 cm<sup>3</sup> K mol<sup>-1</sup> (for compounds **2–6**), respectively. From above-mentioned results it is clear that the central Fe<sup>III</sup> ion in an anhydrous complex **1** is in high-spin state with five unpaired electrons (spin-only value for Fe<sup>III</sup>,  $S = 5/2$ ; 5.92  $\mu_{\text{eff}}/\mu_B$ ) [25]. In all other cases (**2–6**), there is at least one crystal water molecule, which probably enters the vicinity of central atom and subsequently increases the coordination number from 4 to 5. The result of this process is a mixture of complexes with two different geometries (tetrahedron and trigonal-bipyramid) and also possibly two different spin states ( $S = 5/2$  and  $S = 3/2$ ).

Temperature dependence of magnetic susceptibility for two compounds (**1** and **4**) was also measured within the temperature range of 80–298 K (see Fig. 2). It has been found, that the effective magnetic moment value is very smoothly decreased along with decreasing temperature, specifically from 5.80  $\mu_{\text{eff}}/\mu_B$  to 5.70  $\mu_{\text{eff}}/\mu_B$  (for **1**) and from 5.36  $\mu_{\text{eff}}/\mu_B$  to 5.24  $\mu_{\text{eff}}/\mu_B$  (for **4**). The simple Curie–Weiss model was used to determination of parameters such as Curie and Weiss constants. The Curie constant values were found to be 4.350 cm<sup>3</sup> K mol<sup>-1</sup> (for **1**) and 3.717 cm<sup>3</sup> K mol<sup>-1</sup> (for **4**). These values support our assumption of the clear high-spin tetrahedral arrangement for compound **1** (theoretical Curie constant

value for  $S = 5/2$  is 4.377 cm<sup>3</sup> K mol<sup>-1</sup>). The Curie constant value of compound **4** lies between  $S = 3/2$  state (theoretical value 1.876 cm<sup>3</sup> K mol<sup>-1</sup>) and  $S = 5/2$  spin states (see above), which indicates the presence of a spin mixture with  $S = 3/2$  state in minority. Based on the determined Weiss constant values for complexes **1** [ $\theta = -2.7(4)$  cm<sup>-1</sup>] and **4** [ $\theta = -5.2(3)$  cm<sup>-1</sup>], the presence of a weak antiferromagnetic interaction has been found in both cases. It may be connected with variety hydrogen bonds and non-bonding interactions presented within the sample in the solid state. Moreover, the antiferromagnetic interaction may be also indicated by a sextet in low-temperature Mössbauer spectrum of complex **4**. Finally, we may not pronounce the univocal conclusion regarding the stereochemistry and electronic structure, but the results obtained from magnetochemical measurements confirm indirectly our presumption acquired by <sup>57</sup>Fe Mössbauer spectroscopy.

## 2.3. <sup>1</sup>H and <sup>13</sup>C NMR spectroscopies and ES+ mass spectrometry

In an effort to suppress the consequences of paramagnetism of the complexes on the appearance and interpretation of NMR spectra, low concentration of samples for <sup>1</sup>H NMR experiments was used. However, measuring of these low concentration samples resulted in the spectra, where intensities of signals of deuterated solvents are incomparably higher than intensity of signals of the compounds themselves in some cases, and thus, some regions of the spectra were not interpretable. For that reason, various deuterated solvents (DMSO-*d*<sub>6</sub>, MeOH-*d*<sub>3</sub>, DMF-*d*<sub>7</sub>, acetone-*d*<sub>6</sub>) were used for measurements with purpose to suppress these observations and with the effort to find and interpret as many signals as possible. The use of different deuterated solvents also proved indirectly a stability of measured compounds in the solution, because the corresponding spectra were found to be identical in time dependent experiments. In <sup>1</sup>H NMR spectra, the most significant coordination shifts,  $\Delta\delta$ , were found in the case of the C8–H signals ( $\Delta\delta = 0.29$ – $0.50$  ppm;  $\Delta\delta = \delta_{\text{complex}} - \delta_{\text{ligand}}$ ). As for <sup>13</sup>C NMR spectra, the most significant coordination shifts were found for the C8 ( $\Delta\delta = 3.51$ – $3.61$  ppm) and C5 atoms [ $\Delta\delta = -2.58$ –( $-6.26$  ppm)]. In relation to above-mentioned results we assume the

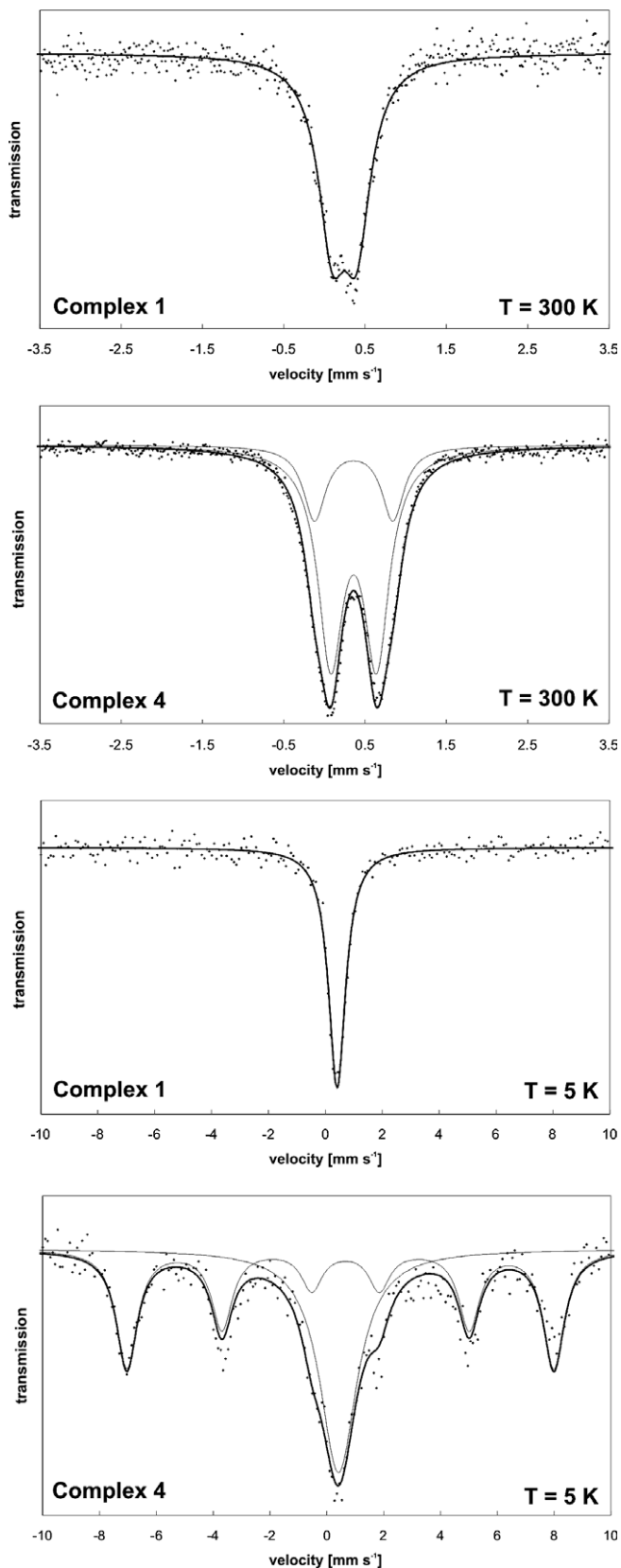


Fig. 1.  $^{57}\text{Fe}$  Mössbauer spectra of complexes **1** and **4** taken at temperatures of 300 and 5 K, together with the fitted subspectra. Full lines represent the best fit.

coordination of organic ligand to  $\text{Fe}^{\text{III}}$  ion through nitrogen atom N7, which is also the most possible coordination site due to steric

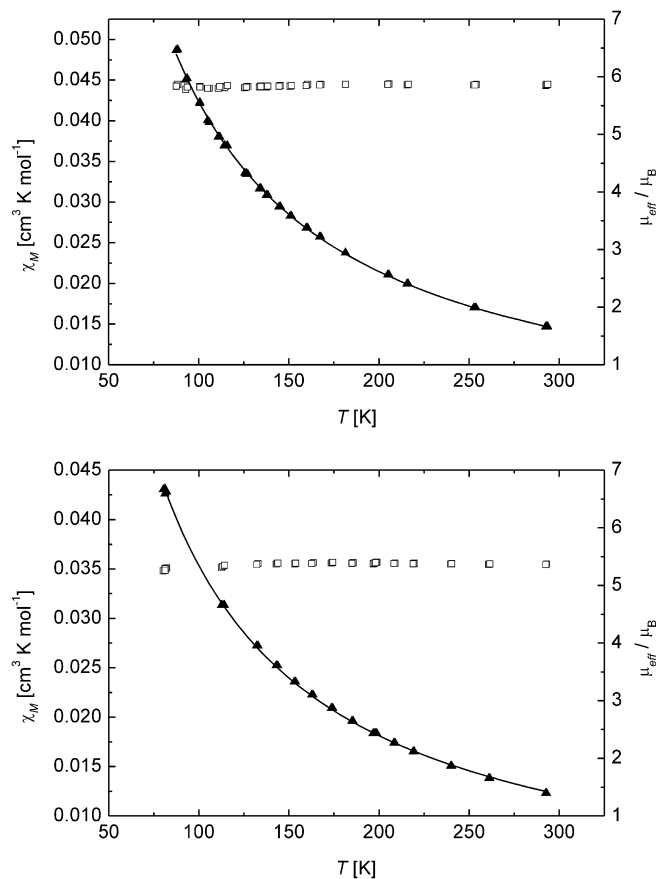


Fig. 2. Temperature dependence of the molar magnetic susceptibility (full triangles) and the effective magnetic moment (squares) for complex **1** (up) and complex **4** (down); full lines – fitted data.

hindrance of N1 and N3 sites caused by substitution of purine skeleton at C2, C6 and N9 positions.

ES+ mass spectra were measured for complexes **1–6**. The  $[\text{M}+\text{H}]^+$  molecular peak of the complexes, without molecules of crystal water, appeared at 549 (for **2**), 568 (for **3**), 525 (for **5**) and 568  $m/z$  (for **6**). Consecutively, the peaks observed at 359 (for **1**), 385 (for **2**), 371 (for **3**), 355 (for **4**), 327 (for **5**) and 387  $m/z$  (for **6**) clearly indicate the presence of the appropriate organic ligand  $\text{L}_n$  in the complexes. The peak located at 513 (for **2**), 483 (for **4**) and 454  $m/z$  (for **5**) can be assigned to  $[\text{Fe}(\text{L}_n)\text{Cl}_2+\text{H}]^+$  fragment, whilst peak at 461 (for **3**), 445 (for **4**), 417 (for **5**) and 477  $m/z$  (for **6**) probably belongs to fragment of  $[\text{Fe}(\text{L}_n)\text{Cl}+\text{H}]^+$ . The molecules of organic ligands were also fragmented and the peaks at 137  $m/z$  are connected with  $[\text{adenine}+\text{H}]^+$ .

#### 2.4. IR spectra

IR spectra of the complexes **1–6** were measured over the range of 150–4000  $\text{cm}^{-1}$  (see Table 2). The bands observed between 1634 and 1638  $\text{cm}^{-1}$  may be assigned to the  $\nu(\text{C}=\text{N})$  stretch vibration of the heterocyclic rings. The same bands appear in the spectra of the free CDK inhibitors, but near value of 1620  $\text{cm}^{-1}$ , which can support the coordination of the organic ligands through any N-atom of a purine moiety to  $\text{Fe}^{\text{III}}$  central cation. The bands observed at 1572–1581 and 1420–1450  $\text{cm}^{-1}$  correspond to  $\nu(\text{C}=\text{C})$  vibration of aromatic rings, while peaks observed in the region of 640–920  $\text{cm}^{-1}$  are assignable to skeletal vibration of the purine ring [26]. The maximum near 1050  $\text{cm}^{-1}$  is observable in the spectra of complexes **2–6**, and can be assigned to  $\nu(\text{C}_{\text{all}}-\text{O})$  vibration of a

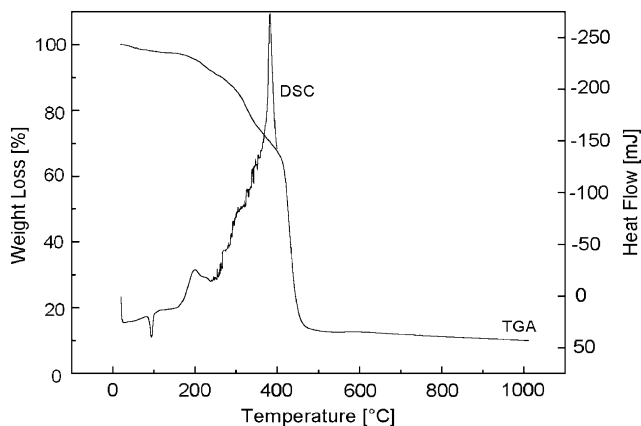


Fig. 3. TGA and DSC curves of complex **2**.

primary alcoholic group [27]. In the spectra of complexes **2**, **3**, and **6**, the maximum about  $1214\text{ cm}^{-1}$  was also found, which can be assigned to  $\nu(\text{C}_{\text{ar}}-\text{O})$  vibration of hydroxyl group attached to a ben-

zene ring [27]. Spectrum of compound **1** showed two maxima at  $753$  and  $658\text{ cm}^{-1}$  assignable to  $\nu(\text{C}_{\text{alif}}-\text{Cl})$  vibration [27]. The bands of  $\delta(\text{CH}_2)$  are located in the range of  $1482$ – $1496\text{ cm}^{-1}$  in the spectra of all compounds. All the above-mentioned vibrational maxima observed in the infrared spectra clearly proved the presence of the corresponding  $\text{L}_n$  ligand in compounds **1**–**6**. The maxima, which appeared in spectra of all complexes near  $3100$  and  $3400\text{ cm}^{-1}$ , can be assigned to the  $\nu(\text{C}-\text{H})_{\text{ar}}$ , and  $\nu(\text{N}-\text{H})$  or  $\nu(\text{O}-\text{H})$  vibrations, respectively [27,28]. A very strong band observed near  $382\text{ cm}^{-1}$  can be clearly assigned to  $\nu(\text{Fe}-\text{Cl})$  vibration [28,29]. There is one more band of a weak intensity near  $334\text{ cm}^{-1}$ , which based on the literature data [29], may be assigned to the  $\nu(\text{Fe}-\text{N})$  stretching vibration.

### 2.5. Thermal analysis

The thermal behaviour of the prepared complexes can be demonstrated on the complex **2**  $\{[\text{Fe}(\text{L}_2)\text{Cl}_3]\cdot\text{H}_2\text{O}\}$  (Fig. 3). The course of the thermal decompositions for all compounds are very similar, however, in the case of **2**, the first weight decrease proceeds in

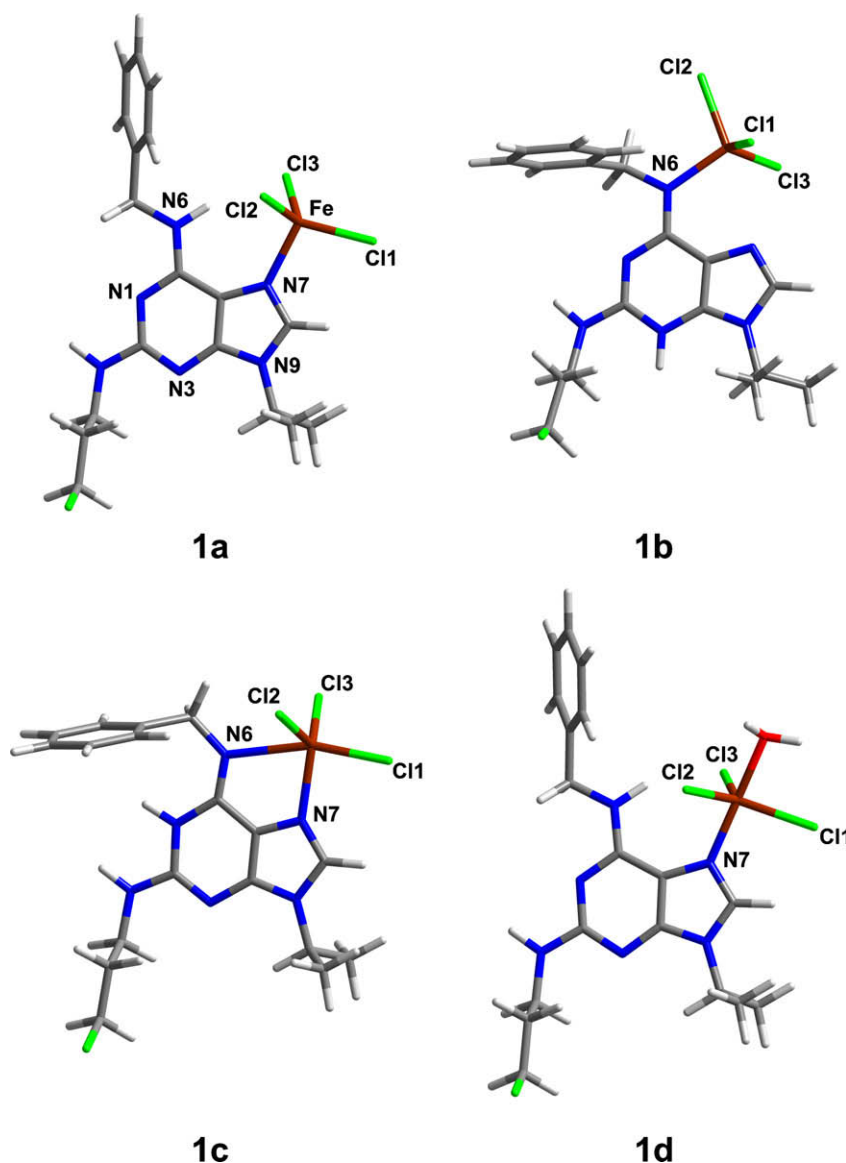


Fig. 4. The geometries of possible structures of complex **1**,  $[\text{Fe}(\text{L}_1)\text{Cl}_3]$  ( $S = 5/2$ ) **1a**–**1c** and  $[\text{Fe}(\text{L}_1)\text{Cl}_3(\text{H}_2\text{O})]$  ( $S = 3/2$ ) **1d**, optimized on the B3LYP/6-311+G/Wachter's level of theory.

the temperature range of 41–140 °C and can be connected with the elimination of one crystal water molecule (found/calcd.: 2.8/3.0%). This process is accompanied by an endothermic effect on the DSC curve with the minimum at 93.7 °C ( $\Delta H = 54.6 \text{ mJ} = 10.3 \text{ kJ mol}^{-1} = 2.5 \text{ kcal mol}^{-1}$ ). Further, the compound exists as an anhydrous intermediate between temperatures of 141 and 158 °C. The main thermal decomposition of the studied complex starts at 159 °C and proceeds in two steps without formation of stable intermediates. The first step can be observed on the TGA curve in the temperature range of 159–248 °C and is accompanied by a broad exothermic effect on the DSC curve, with the maximum at 199.3 °C ( $\Delta H = -75.3 \text{ mJ} = -14.2 \text{ kJ mol}^{-1} = 3.4 \text{ kcal mol}^{-1}$ ). The second step, i.e. main weight decrease, of thermal decomposition appeared in the range of 273–503 °C and is associated with intensive and sharp exothermic effect with the maximum at 386 °C. The total weight decrease (87.0%) is in a good correspondence with the calculated value of 86.1% and is clearly connected with decomposition of the complex to  $\alpha\text{-Fe}_2\text{O}_3$  which was proved using  $^{57}\text{Fe}$  Mössbauer spectroscopy ( $\delta = 0.37 \text{ mm s}^{-1}$ ,  $\Delta E_Q = 0.21 \text{ mm s}^{-1}$ , hyperfine magnetic field 51.2 T).

## 2.6. Quantum chemical calculations

The complex of  $[\text{Fe}(\text{L}_1)\text{Cl}_3]$  (**1**) has been chosen as a model system for the quantum chemical investigation of the geometry and electronic structure of iron compounds presented in this work. In general, there are two different possibilities how the  $\text{L}_1$  ligand can be coordinated to  $\text{Fe}^{\text{III}}$  ion: (i) a monodentate coordination via N1, N3 or N7 atom; (ii) a bidentate coordination via N6 and N7 atoms. The questions regarding the spin state of the iron(III) central ion in connection with stereochemistry of the complex had to be also taken into account during the calculations. Optimized molecular geometries of the complex **1** are shown in Fig. 4, their important structural data are summarized in Table 4.

Based on the above-mentioned results (Fig. 4, Table 4), and moreover, taking into account a steric hindrance of some possible coordination sites of the  $\text{L}_1$  ligand (both N1 and N3 binding sites are sterically hindered by adjacent substituents at C2 and N9 positions – for better view, see the Fig. 4), may be concluded that only ligand's coordination via N7 or both N7 and N6 atom should lead to the complex formation.

The results obtained by magnetic susceptibility measurements and  $^{57}\text{Fe}$  Mössbauer spectroscopy indicated the presence of two spin states (with  $S = 5/2$  and  $S = 3/2$ ) within the complexes **2–6**, which may originate from different geometries of the complexes. The geometry each of the hydrated complexes **2–6** may be influenced by two main manners. The first way may be related with fact that either one crystal water molecule may enter to the inner coordination sphere of the central iron atom or the corresponding organic ligand,  $\text{L}_n$ , may be coordinated as a bidentate one probably through the N6 and N7 atoms. On the other hand, the complex **1** can be considered to be magnetically and structurally "pure", because nearly the spin-only effective magnetic moment value ( $5.82 \mu_{\text{eff}}/\mu_{\text{B}}$ ) was determined in this case, and thus, its geometry can be described as a distorted tetrahedron (based on  $^{57}\text{Fe}$  Mössbauer data and DFT geometry optimizations).

As can be seen from the Fig. 4, the monodentate ligand's coordination to the  $\text{Fe}^{\text{III}}$  ion involving the  $5/2$  spin state leads to the formation of stable complex **1a** with tetrahedral arrangement of the coordination sphere (structure **1a**), while the monodentate coordination via the N6 or N7 atom requires, as a first step, to shift the N6-H proton to any other of non-substituted nitrogen atoms of the purine moiety (i.e. N1 or N3) – see the structure **1b**. However, such rearrangement necessarily leads to the disruption of the  $\pi$ -electron delocalization within the purine ring, which may result in decreasing of the molecular system stability.

Thus,  $\Delta G$  of the complex involving the N3 protonated and N6 coordinated ligand (**1b**) is by  $33.2 \text{ kcal mol}^{-1}$  higher as compared to that of the complex **1a**. If the ligand is bidentate coordinated via the N6 and N7 atoms and the proton is shifted to the N1 position, then the molecular structure is partially stabilized by weak interaction between mentioned proton and  $\pi$ -electron system of the benzyl moiety. In this case, the geometry of the complex can be described as a distorted trigonal-bipyramid (structure **1c**). Nevertheless, the  $\Delta G$  energy of such complex is increased by  $13.6 \text{ kcal mol}^{-1}$  as compared to that of structure **1a**. As for the structure **1d**, the coordination number of iron is increased by the coordination of one water molecule, and thus, the donor atoms arrangement of the structure has a shape of trigonal-bipyramid (structure **1d**).

In quest of interpret infrared spectra of the compounds, the calculation of vibrational frequencies for the complex **1a** at the B3LYP/6-311+G/Wachter's level of the theory has been also performed. The calculated infrared spectrum of the complex **1a** shows two strong bands in the far IR region at  $403$  and  $411 \text{ cm}^{-1}$ , which are assignable to the  $\nu(\text{Fe-Cl})$  vibration. The stretching vibration of  $\nu(\text{Fe-N})$  has been found at  $344 \text{ cm}^{-1}$ . All these values correspond well with experimental data (for details, see Table 2). For a comparison, the vibrational frequencies of the complexes **1c** and **1d** were also calculated. The calculated spectrum of the complex **1c** showed bands belonging to the  $\nu(\text{Fe-Cl})$  vibration at  $383$  and  $412 \text{ cm}^{-1}$ , while maximum attributable to the  $\nu(\text{Fe-N})$  vibration has been found at  $192 \text{ cm}^{-1}$ . Similarly, the  $\nu(\text{Fe-Cl})$  vibrations of the complex **1d** have been found at  $378$  and  $407 \text{ cm}^{-1}$ , and the  $\nu(\text{Fe-N})$  one at  $199 \text{ cm}^{-1}$ .

The calculated values of Mössbauer shift,  $\delta$ , was found to be  $0.364 \text{ mm s}^{-1}$  for a tetrahedral structure of **1a** ( $S = 5/2$ ) and  $0.450 \text{ mm s}^{-1}$  for a trigonal-bipyramidal structure of **1d** ( $S = 3/2$ ). However, it is necessary to note at this moment that the calculations were performed at 0 K and vacuum, thus the value of the temperature Doppler shift (ca.  $0.10\text{--}0.12 \text{ mm s}^{-1}$  for Fe-complexes) has to be applied to correct the corresponding values to the values at room temperature. We may conclude after the realization of these corrections that the calculated values correspond well with those of experimentally obtained (see Table 3).

## 2.7. Biological activity testing

*In vitro* antitumour activity of all prepared complexes **1–6** and the starting compounds  $\text{L}_1\text{--L}_6$  and  $\text{FeCl}_3 \cdot 6\text{H}_2\text{O}$  have been determined. The results of biological testing are presented in Table 5. With the exception of **1**, all the prepared complexes showed a substantial activity in a micromolar range on human malignant melanoma (G-361), osteogenic sarcoma (HOS), chronic myelogenous leukaemia (K-562) and breast adenocarcinoma cell line (MCF-7). The comparison of  $\text{IC}_{50}$  values of the iron complexes **1–6** with the respective free ligands  $\text{L}_1\text{--L}_6$  demonstrates that the complex formation has no significant impact on the resulting *in vitro* cytotoxicity. From the above results we may draw conclusion that the ability of the complexes to decrease number of viable cells, as compared to free ligands  $\text{L}_1\text{--L}_6$ , is probably caused by the presence of the organic ligands themselves within the complexes. On the other hand, the  $\text{IC}_{50}$  values obtained on the MCF-7 cell line in the case of complexes **2** and **3** are even better than those of Cisplatin and Oxaliplatin (see Table 5), i.e. widely used platinum-based anticancer drugs. However, it is necessary to note at this point that partial hydrolysis and dissociation of the iron complexes should proceed under both *in vitro* and *in vivo* conditions. Based on NMR results (more specifically on the  $^1\text{H}$  and  $^{13}\text{C}$  NMR coordination shift values) it may be concluded that the appropriate  $\text{L}_n$  organic ligand behaves as an *N*-donor carrier ligand in all the

**Table 4**  
Selected interatomic parameters (Å, °) of the studied complexes calculated on the B3LYP/6-311+G/Wachter's level.

	1a	1b	1c	1d	1a, exp.	1d, exp.
Fe–Cl1	2.204	2.222	2.262	2.307	2.259 <sup>a</sup>	2.392 <sup>b</sup>
Fe–Cl2	2.198	2.228	2.235	2.273		
Fe–Cl3	2.209	2.217	2.226	2.243		
Fe–N7	2.074	3.044	2.155	1.955	2.106 <sup>a</sup>	2.182 <sup>b</sup>
Fe–N6	–	2.092	2.536	–		
Fe–O	–	–	–	2.017		2.135 <sup>b</sup>
Cl1–Fe–Cl2	114.06	105.72	103.81	120.01		
Cl1–Fe–Cl3	114.37	119.75	104.25	114.28		
Cl2–Fe–Cl3	112.67	105.95	117.43	124.69		
N7–Fe–Cl1	104.04	–	89.33	95.97		
N7–Fe–Cl2	105.06	–	117.46	90.89		
N7–Fe–Cl3	105.32	–	117.58	93.45		
N6–Fe–Cl1	–	109.60	84.05	–		
N6–Fe–Cl2	–	103.73	85.06	–		
N6–Fe–Cl3	–	110.68	73.36	–		
N6–Fe–N7	–	–	162.67	–		
Cl1–Fe–O	–	–	–	83.50		
Cl2–Fe–O	–	–	–	85.18		
Cl3–Fe–O	–	–	–	91.20		
N7–Fe–O	–	–	–	175.10		

*T<sub>d</sub>*, tetrahedral; *TB*, trigonal–bipyramidal.

<sup>a</sup> The values represent mean values which were determined from known X-ray structures of complexes bearing *T<sub>d</sub>* FeCl<sub>3</sub>N chromophore and are deposited within the Cambridge Crystallographic Data Centre (CSD).

<sup>b</sup> The values represent mean values which were determined from known X-ray structures of complexes bearing *TB* FeCl<sub>3</sub>NO chromophore and are deposited within the Cambridge Crystallographic Data Centre (CSD).

**Table 5**

IC<sub>50</sub> values, given together with their standard deviations, assessed by calcein AM assay of surviving tumour cells and IC<sub>50</sub> values for inhibition of Cdk2/cyclin E kinase (both in μM).

Compound	IC <sub>50</sub> (μM)				
	<i>G-361</i>	<i>HOS</i>	<i>K-562</i>	<i>MCF-7</i>	<i>CDK2/E</i>
[Fe(L <sub>1</sub> )Cl <sub>3</sub> ] (1)	>50	>50	>50	>50	1.50 ± 0.41
L <sub>1</sub>	>100	>100	>100	>100	1.05 ± 0.32
[Fe(L <sub>2</sub> )Cl <sub>3</sub> ]·H <sub>2</sub> O (2)	4 ± 1	7 ± 1	12 ± 1	5 ± 1	0.11 ± 0.02
L <sub>2</sub>	5 ± 1	8 ± 1	9 ± 1	2 ± 1	0.07 ± 0.02
[Fe(L <sub>3</sub> )Cl <sub>3</sub> ]·2H <sub>2</sub> O (3)	15 ± 3	10 ± 2	21 ± 4	6 ± 2	0.05 ± 0.02
L <sub>3</sub>	29 ± 7	10 ± 2	21 ± 3	7 ± 4	0.20 ± 0.11
[Fe(L <sub>4</sub> )Cl <sub>3</sub> ]·2H <sub>2</sub> O (4)	15 ± 2	23 ± 4	>50	12 ± 2	0.09 ± 0.02
L <sub>4</sub>	19 ± 2	20 ± 3	50 ± 4	15 ± 2	0.20 ± 0.06
[Fe(L <sub>5</sub> )Cl <sub>3</sub> ]·2H <sub>2</sub> O (5)	>50	>50	>50	43 ± 8	0.48 ± 0.08
L <sub>5</sub>	135 ± 18	120 ± 24	118 ± 21	61 ± 16	2.05 ± 0.49
[Fe(L <sub>6</sub> )Cl <sub>3</sub> ]·2H <sub>2</sub> O (6)	33 ± 5	41 ± 4	55 ± 8	23 ± 4	0.02 ± 0.01
L <sub>6</sub>	48 ± 8	68 ± 5	65 ± 11	12 ± 2	0.07 ± 0.03
FeCl <sub>3</sub> ·6H <sub>2</sub> O	>200	>200	>200	>200	–
Cisplatin	3	3	5	11	–
Oxaliplatin	7	7	9	18	–

The tumour cell lines (*G-361*, human malignant melanoma; *HOS*, human osteogenic sarcoma; *K-562*, human chronic myelogenous leukaemia; *MCF-7*, human breast adenocarcinoma) were treated with solution of the tested compounds in the 0.5–50 μM, 0.5–100 μM, and 0.5–200 μM ranges, respectively, for 72 h.

complexes, i.e. it remains coordinated to the iron(III) cation in a solution. It should also be mentioned that the NMR experiments were performed under strictly non-biological conditions, i.e. in solvents such as DMSO-*d*<sub>6</sub>, MeOH-*d*<sub>3</sub>, DMF-*d*<sub>7</sub>, acetone-*d*<sub>6</sub>, and thus, the interpretation given above would not be valid in the case of experiments running under biological conditions. On the other hand, it is also highly probable that the three chlorido ligands

represent a leaving group in *in vitro* tests. Thus, we believe that under physiological conditions, the hydrolysis and dissociation of the iron(III) complexes **1–6** should proceed in a much greater rate and the complexes should be present there in the forms of the [Fe(L<sub>*n*</sub>)(OH)Cl<sub>2</sub>], [Fe(L<sub>*n*</sub>)(OH)<sub>2</sub>Cl] and/or [Fe(L<sub>*n*</sub>)(OH)<sub>3</sub>] species, and moreover, a sizable amount of free CDK-inhibitor L<sub>*n*</sub> should also be present within the system as a consequence of the dissociation of the complexes. Taking all the above said into consideration, it may be concluded that just the mentioned processes might be a cause of the obtained IC<sub>50</sub> values for the complexes **1–6**, as compared to free ligands L<sub>1–6</sub>.

The inhibition of recombinant human cyclin E/Cdk2 kinase by all the complexes and free ligands was also determined. The results, summarized in Table 5, proved the ability of all tested complexes to inhibit the activity of this important cell cycle regulating protein kinase. The most potent complexes **3** and **6** even reached a low submicromolar range of efficiency. To our best knowledge, the complexes **2–6** have been found to be the most active cyclin E/CDK2 inhibitors based on transition metal complexes, and moreover, they were found to be quite comparable to and even better than other CDK inhibitors involving the 6-benzylaminopurine moiety [9]. It may be concluded that the coordination of the appropriate L<sub>3</sub>, L<sub>4</sub>, L<sub>5</sub> and L<sub>6</sub> molecules to Fe<sup>III</sup> ion led to the formation of complexes for which the determined inhibitory effect is significantly higher as compared to the free ligands. However, it should also be noted here that a partial hydrolysis and dissociation have to be taken into account in the case of interpretation of the IC<sub>50</sub> values regarding the inhibitory activity, similarly as it was mentioned above as for the cytotoxicity results.

## 2.8. X-ray structure of 2-chloro-6-benzylamino-9-isopropylpurine

The molecular structure of 2-chloro-6-benzylamino-9-isopropylpurine, i.e. an intermediate for the preparation of L<sub>1</sub>, L<sub>4</sub> and L<sub>5</sub>, is shown in Fig. 4. There are two molecules in the crystallographically independent part. The crystal structure is stabilized by N<sub>amino</sub>–H...N<sub>purine</sub> hydrogen bonds connecting two adjacent molecules, thus forming centrosymmetric dimers (Fig. 5). Each of two molecules contains nearly planar benzene (A), pyrimidine (B) and imidazole (C) ring systems, with maximum deviations from each plane of 0.005(2) (C14) and 0.003(2) Å (C13A) for rings A, 0.006(2) (C6) and 0.013(2) Å (C4A) for six-membered rings B, and 0.004(2) (C5) and 0.001(2) Å (C4A) for five-membered rings C [30]. Atoms forming the purine rings (B+C) deviate slightly from planarity, with the greatest deviation being 0.009(2) and 0.034(2) Å for atom C6, and C5A, respectively. Planes B and C are nearly coplanar, with a dihedral angle of 0.29(6)°, and 2.79(9)°, respectively, whilst the dihedral angles between plane A and the purine ring (B+C) are 84.45(6)°, and 80.50(6)°, respectively. The Cg1...Cg2, Cg1...Cg3 and Cg2...Cg3 distances are 5.8110(1), 6.7861(2), and 2.0768(1) Å, respectively, where Cg1, Cg2 and Cg3 are the centroids of rings A, B, and C, respectively. The values of the same centroid-to-centroid distances for the second molecule are 5.7798(2), 6.8701(2) and 2.0764(1) Å. The torsion angles C6–N6–C9–C10, C9–N6–C6–C5 and N6–C9–C10–C15, C6–N6–C9–C10, C9–N6–C6–C5 and N6–C9–C10–C15 are 109.6(2), –178.4(2) and 148.2(2)° for the first molecule and 108.5(2)°, 171.2(2)° and –39.6(3)° for the second one, respectively.

It has been found that bond lengths and angles within the two crystallographically independent molecules of 2-chloro-6-benzylamino-9-isopropylpurine, L, do not differ significantly each other, and moreover, they are consistent with standard values. For this reason, they are summarized in Appendix A as the Supplementary data.

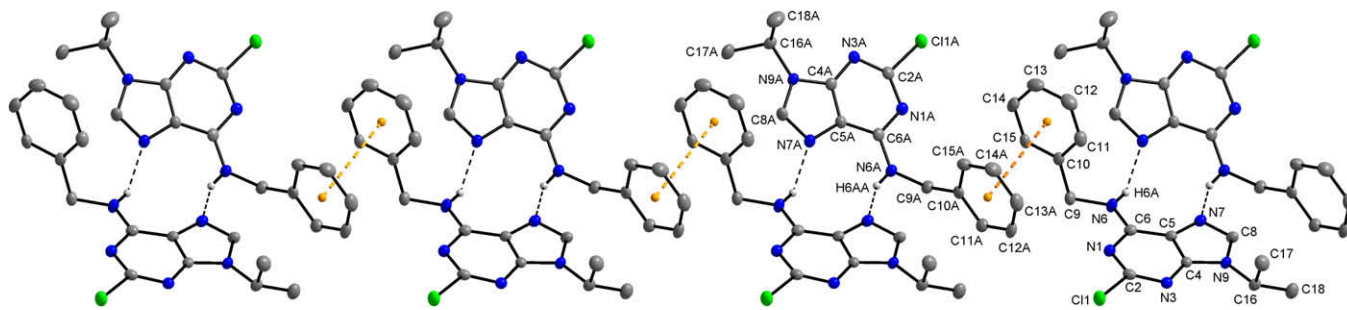


**Fig. 5.** A part of the crystal structure of 2-chloro-6-benzylamino-9-isopropylpurine, i.e. a precursor for the preparation of **L**<sub>1</sub>, **L**<sub>4</sub> and **L**<sub>5</sub>, showing the formation of centrosymmetric dimers, N–H...N hydrogen bonds (dashed lines) and  $\pi$ – $\pi$  stacking interactions (orange dashed lines). Atoms of the two crystallographically independent molecules within the unit cell are numbered only.

### 3. Experimental

#### 3.1. Materials

FeCl<sub>3</sub>·6H<sub>2</sub>O, K<sub>2</sub>CO<sub>3</sub>, 2,6-dichlorpurine, *i*-propylbromide, benzylamine, 2-hydroxy-5-methyl-benzylamine, 3-hydroxy-benzylamine, 3,5-dihydroxy-benzylamine and solvents used were purchased from Fluka or Aldrich Co. and were used without further purification.

#### 3.2. Preparation of ligands **L**<sub>1</sub>–**L**<sub>6</sub>

The CDK inhibitors, used as ligands **L**<sub>1</sub>–**L**<sub>6</sub> in this study, were prepared by a slightly modified method described earlier [31]. A general pathway for the preparation of the free ligands is depicted in Scheme 3. The purity of the compounds was checked by elemental analyses, <sup>1</sup>H and <sup>13</sup>C NMR spectroscopy and thin-layer chromatography (TLC). The splitting of proton resonances in the reported <sup>1</sup>H spectra is defined as s = singlet, d = doublet, t = triplet, q = quartet, qui = quintet, sxt = sextet, sep = septet, bs = broad signal, dd = doublet of doublets, tt = triplet of triplets, m = multiplet.

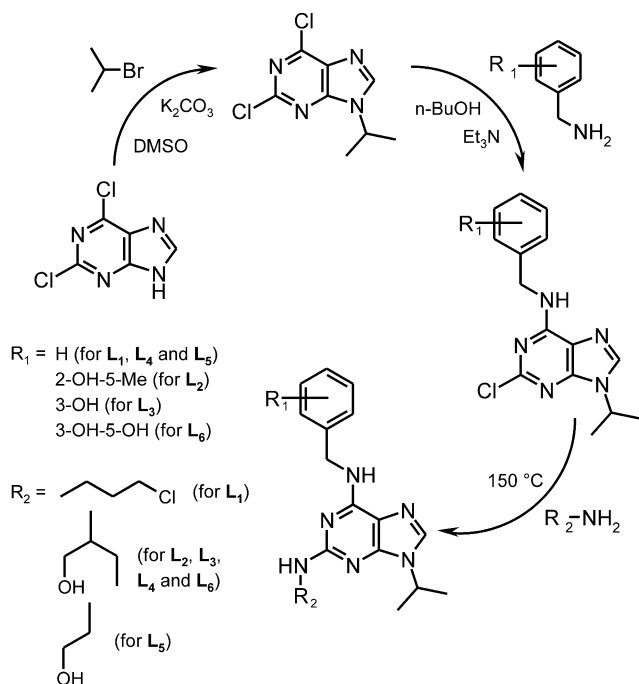
**L**<sub>1</sub>: Yield: ~60%; Anal. Calc. for C<sub>18</sub>H<sub>23</sub>N<sub>6</sub>Cl<sub>1</sub>: C, 60.3; H, 6.4; N, 23.4. Found: C, 60.0; H, 6.6; N, 23.2%. <sup>1</sup>H NMR (DMF-*d*<sub>7</sub>, ppm): 7.67 (bs, 1H, (N6)H), 7.79 (s, 1H, (C8)H), 7.45 (d, 2H, (C11,15)H, *J* = 7.2 Hz), 7.31 (tt, 2H, (C12,14)H, *J*<sub>a</sub> = 7.5 Hz, *J*<sub>b</sub> = 1.7 Hz), 7.22 (tt, 1H, (C13)H, *J*<sub>a</sub> = 7.3 Hz, *J*<sub>b</sub> = 1.8 Hz), 6.41 (t, 1H, (N2)H, *J* = 5.8 Hz), 4.80 (s, 2H, (C9)H), 4.63 (sep, 1H, (C16)H, *J* = 6.8 Hz), 3.72 (t, 2H, (C21)H, *J* = 6.6 Hz), 3.50 (qui, 2H, (C19)H, *J* = 6.6 Hz), 2.07 (qui, 2H, (C20)H, *J* = 6.6 Hz), 1.53 (d, 6H, (C17,18)H, *J* = 6.8 Hz). <sup>13</sup>C NMR (DMF-*d*<sub>7</sub>, ppm): 160.27 (C2), 155.73 (C6), 151.92 (C4), 135.80 (C8), 141.82 (C10), 128.80 (C12,14), 128.22 (C11,15), 127.19 (C13), 115.06 (C5), 60.12 (C20), 46.82 (C16), 44.11 (C19), 39.64 (C9), 33.70 (C21), 22.40 (C17,18). TLC: one spot.

**L**<sub>2</sub>: Yield: ~70%; Anal. Calc. for C<sub>20</sub>H<sub>28</sub>N<sub>6</sub>O<sub>2</sub>: C, 62.5; H, 7.3; N, 21.9. Found: C, 62.5; H, 7.5; N, 21.9%. <sup>1</sup>H NMR (DMSO-*d*<sub>6</sub>, ppm): 9.68 (s, 1H, (O2)H), 7.79 (s, 1H, (C8)H), 7.43 (bs, 1H, (N6)H), 6.99 (d, 1H, (C15)H, *J* = 2.1 Hz), 6.85 (dd, 1H, (C13)H, *J*<sub>a</sub> = 8.1 Hz, *J*<sub>b</sub> = 2.1 Hz), 6.67 (d, 1H, (C12)H, *J* = 8.1 Hz), 5.84 (d, 1H, (N2)H, *J* = 8.1 Hz), 4.59 (s, 1H, (O1)H), 4.53 (sep, 1H, (C16)H, *J* = 6.8 Hz), 4.58 (s, 2H, (C9)H), 3.82 (m, 1H, (C19)H), 3.48 (qui, 1H, (C20)H<sub>a</sub>, *J* = 5.3 Hz), 3.41 (m, 1H, (C20)H<sub>b</sub>), 2.14 (s, 3H, (C23)H), 1.62 (sep, 1H, (C21)H<sub>a</sub>, *J* = 7.3 Hz), 1.48 (m, 1H, (C21)H<sub>b</sub>), 1.47 (dd, 6H, (C17,18)H, *J*<sub>a</sub> = 6.8 Hz, *J*<sub>b</sub> = 2.3 Hz), 0.86 (q, 3H, (C22)H, *J* = 7.3 Hz). <sup>1</sup>H NMR (MeOH-*d*<sub>3</sub>, ppm): 7.77 (s, 1H, (C8)H), 7.07 (s, 1H, (C15)H), 6.92 (d, 1H, (C13)H, *J* = 8.2 Hz), 6.70 (d, 1H, (C12)H, *J* = 8.2 Hz), 4.61 (s, 2H, (C9)H), 4.66 (m, 1H, (C16)H), 4.00 (m, 1H, (C19)H), 3.66 (dd, 2H, (C20)H, *J*<sub>a</sub> = 5.1 Hz, *J*<sub>b</sub> = 2.0 Hz), 2.21 (s, 3H, (C23)H), 1.74 (sep, 1H, (C21)H<sub>a</sub>, *J* = 7.3 Hz), 1.61 (m, 1H, (C21)H<sub>b</sub>), 1.55 (d, 6H, (C17,18)H, *J* = 6.8 Hz), 1.01 (t, 3H, (C22)H, *J* = 7.3 Hz). <sup>1</sup>H NMR (acetone-*d*<sub>6</sub>, ppm): 10.51 (s, 1H (O2)H), 7.24 (bs, 1H,

(N6)H), 7.67 (s, 1H, (C8)H), 7.11 (s, 1H, (C15)H), 6.92 (dd, 1H, (C13)H, *J*<sub>a</sub> = 8.1 Hz, *J*<sub>b</sub> = 2.1 Hz), 6.69 (d, 1H, (C12)H, *J* = 8.1 Hz), 5.43 (d, 1H, (N2)H, *J* = 8.1 Hz), 4.53 (s, 1H, (O1)H), 4.58 (s, 2H, (C9)H), 4.62 (sep, 1H, (C16)H, *J* = 6.8 Hz), 4.01 (m, 1H, (C19)H), 3.69 (m, 2H, (C20)H), 2.20 (s, 3H, (C23)H), 1.77 (sep, 1H, (C21)H<sub>a</sub>, *J* = 7.3 Hz), 1.67 (sep, 1H, (C21)H<sub>b</sub>, *J* = 7.3 Hz), 1.53 (d, 6H, (C17,18)H, *J* = 6.8 Hz), 1.00 (t, 3H, (C22)H, *J* = 7.3 Hz). <sup>1</sup>H NMR (DMF-*d*<sub>7</sub>, ppm): 10.21 (bs, 1H, (O2)H), 7.58 (s, 1H, (N6)H), 7.82 (s, 1H, (C8)H), 7.12 (d, 1H, (C15)H, *J* = 2.1 Hz), 6.91 (dd, 1H, (C13)H, *J*<sub>a</sub> = 8.1 Hz, *J*<sub>b</sub> = 2.1 Hz), 6.75 (d, 1H, (C12)H, *J* = 8.1 Hz), 5.86 (d, 1H, (N2)H, *J* = 8.2 Hz), 4.80 (bs, 1H, (O1)H), 4.67 (s, 2H, (C9)H), 4.62 (sep, 1H, (C16)H, *J* = 6.8 Hz), 4.01 (m, 1H, (C19)H), 3.66 (m, 2H, (C20)H), 2.18 (s, 3H, (C23)H), 1.77 (sep, 1H, (C21)H<sub>a</sub>, *J* = 7.3 Hz), 1.65 (sep, 1H, (C21)H<sub>b</sub>, *J* = 7.3 Hz), 1.53 (d, 6H, (C17,18)H, *J* = 6.8 Hz), 0.97 (t, 3H, (C22)H, *J* = 7.3 Hz). <sup>13</sup>C NMR (DMSO-*d*<sub>6</sub>, ppm): 159.28 (C2), 154.93 (C6), 153.21 (C11), 151.00 (C4), 135.74 (C8), 129.80 (C14), 128.62 (C15), 127.53 (C13), 126.40 (C10), 115.70 (C12), 114.08 (C5), 63.48 (C20), 54.52 (C19), 46.28 (C16), 24.37 (C21), 22.51 (C17,18), 20.67 (C23), 11.09 (C22).

**L**<sub>3</sub>: Yield: ~65%; Anal. Calc. for C<sub>19</sub>H<sub>26</sub>N<sub>6</sub>O<sub>2</sub>: C, 61.6; H, 7.0; N, 22.7. Found: C, 61.4; H, 7.2; N, 22.5%. <sup>1</sup>H NMR (DMSO-*d*<sub>6</sub>, ppm): 9.21 (s, 1H, (O2)H), 7.77 (s, 1H, (C8)H), 7.66 (bs, 1H, (N6)H), 7.06 (t, 1H, (C14)H, *J* = 8.1 Hz), 6.76 (dd, 2H, (C13,15)H, *J*<sub>a</sub> = 7.9 Hz, *J*<sub>b</sub> = 1.5 Hz), 6.58 (tt, 1H, (C11)H, *J*<sub>a</sub> = 8.2 Hz, *J*<sub>b</sub> = 1.7 Hz), 5.80 (d, 1H, (N2)H, *J* = 8.2 Hz), 4.59 (bs, 1H, (O1)H), 4.59 (s, 2H, (C9)H), 4.53 (sep, 1H, (C16)H, *J* = 6.7 Hz), 3.80 (m, 1H, (C19)H), 3.46 (m, 2H, (C20)H), 1.59 (m, 1H, (C21)H<sub>a</sub>), 1.47 (dd, 6H, (C17,18)H, *J*<sub>a</sub> = 6.7 Hz, *J*<sub>b</sub> = 2.2 Hz), 1.43 (m, 1H, (C21)H<sub>b</sub>), 0.84 (t, 3H, (C22)H, *J* = 7.3 Hz). <sup>1</sup>H NMR (MeOH-*d*<sub>3</sub>, ppm): 7.77 (s, 1H, (C8)H), 7.12 (t, 1H, (C14)H, *J* = 7.8 Hz), 6.81 (m, 2H, (C13,15)H), 6.65 (d, 1H, (C11)H, *J* = 8.2 Hz), 4.66 (s, 2H, (C9)H), 4.64 (m, 1H, (C16)H), 3.94 (m, 1H, (C19)H), 3.61 (m, 2H, (C20)H), 1.67 (m, 1H, (C21)H<sub>a</sub>), 1.51 (m, 1H, (C21)H<sub>b</sub>), 1.55 (d, 6H, (C17,18)H, *J* = 6.7 Hz), 0.95 (t, 3H, (C22)H, *J* = 7.3 Hz). <sup>13</sup>C NMR (DMSO-*d*<sub>6</sub>, ppm): 160.27 (C2), 158.55 (C12), 155.68 (C6), 151.77 (C4), 143.15 (C10), 135.68 (C8), 129.69 (C11), 118.77 (C15), 115.05 (C14), 115.70 (C12), 114.90 (C5), 114.18 (C13), 64.52 (C20), 55.29 (C19), 46.81 (C16), 43.77 (C9), 24.91 (C21), 22.34 (C17,18), 10.99 (C22).

**L**<sub>4</sub>: Yield: ~60%; Anal. Calc. for C<sub>19</sub>H<sub>26</sub>N<sub>6</sub>O<sub>1</sub>: C, 64.4; H, 7.4; N, 23.7. Found: C, 64.5; H, 7.5; N, 23.4%. <sup>1</sup>H NMR (DMSO-*d*<sub>6</sub>, ppm): 7.72 (bs, 1H, (N6)H), 7.77 (bs, 1H, (C8)H), 7.36 (dd, 2H, (C11,15)H, *J*<sub>a</sub> = 7.0 Hz, *J*<sub>b</sub> = 1.7 Hz), 7.28 (tt, 2H, (C12,14)H, *J*<sub>a</sub> = 7.3 Hz, *J*<sub>b</sub> = 1.6 Hz), 7.19 (tt, 1H, (C13)H, *J*<sub>a</sub> = 7.0 Hz, *J*<sub>b</sub> = 1.7 Hz), 5.81 (d, 1H, (N2)H, *J* = 8.2 Hz), 4.65 (bs, 2H, (C9)H), 4.52 (sep, 1H, (C16)H, *J* = 6.9 Hz), 4.52 (d, 1H, (O1)H, *J* = 5.4 Hz), 3.80 (m, 1H, (C19)H), 3.46 (sxt, 1H, (C20)H<sub>a</sub>, *J* = 5.4 Hz), 3.37 (sxt, 1H, (C20)H<sub>b</sub>, *J* = 5.4 Hz), 1.60 (m, 1H, (C21)H<sub>a</sub>), 1.46 (dd, 6H, (C17,18)H, *J*<sub>a</sub> = 6.9 Hz, *J*<sub>b</sub> = 2.1 Hz), 1.44 (m, 1H, (C21)H<sub>b</sub>), 0.84 (t, 3H, (C22)H, *J* = 7.3 Hz). <sup>1</sup>H NMR (MeOH-*d*<sub>3</sub>, ppm): 7.76 (s, 1H, (C8)H), 7.66 (s, 1H, (N6)H), 7.36 (dd, 2H, (C11,15)H, *J*<sub>a</sub> = 7.2 Hz, *J*<sub>b</sub> = 1.7 Hz), 7.29



**Scheme 3.** The three-step synthesis of 6-benzylamino-9-isopropylpurine derivatives,  $L_1$ – $L_6$ , used as organic ligands for the preparation of the  $\text{Fe}^{\text{III}}$  complexes 1–6.

(tt, 2H, (C12,14)H,  $J_a = 7.5$  Hz,  $J_b = 1.6$  Hz), 7.21 (tt, 1H, (C13)H,  $J_a = 7.2$  Hz,  $J_b = 1.7$  Hz), 5.55 (d, 1H, (N2)H),  $J = 7.8$  Hz), 4.80 (s, 1H, (O1)H), 4.73 (d, 2H, (C9)H,  $J = 5.7$  Hz), 4.62 (sep, 1H, (C16)H,  $J = 6.9$  Hz), 3.95 (m, 1H, (C19)H), 3.61 (m, 2H, (C20)H), 1.68 (m, 1H, (C21)H<sub>a</sub>), 1.53 (m, 1H, (C21)H<sub>b</sub>), 1.53 (dd, 6H, (C17,18)H,  $J_a = 6.9$  Hz,  $J_b = 1.7$  Hz) 0.95 (t, 3H, (C22)H,  $J = 7.5$  Hz).  $^1\text{H NMR}$  (DMF- $d_7$ , ppm): 7.72 (bs, 1H, (N6)H), 7.77 (s, 1H, C8-H), 7.45 (d, 2H, (C11,15)H,  $J = 7.2$  Hz), 7.30 (tt, 2H, (C12,14)H,  $J_a = 7.5$  Hz,  $J_b = 1.6$  Hz), 7.22 (tt, 1H, (C13)H,  $J_a = 7.0$  Hz,  $J_b = 1.7$  Hz), 5.86 (d, 1H, (N2)H,  $J = 8.2$  Hz), 4.84 (s, 1H, (O1)H), 4.79 (t, 2H, (C9)H,  $J = 5.2$  Hz), 4.61 (sep, 1H, (C16)H,  $J = 6.9$  Hz), 3.98 (m, 1H, (C19)H), 3.66 (m, 1H, (C20)H<sub>a</sub>), 3.60 (m, 1H, (C20)H<sub>b</sub>), 1.73 (m, 1H, (C21)H<sub>a</sub>), 1.52 (d, 6H, (C17,18)H,  $J = 6.9$  Hz), 1.60 (m, 1H, (C21)H<sub>b</sub>), 0.94t, 3H, (C22)H,  $J = 7.3$  Hz).  $^{13}\text{C NMR}$  (DMF- $d_7$ , ppm): 160.31 (C2), 155.70 (C6), 151.85 (C4), 141.72 (C10), 135.74 (C8), 128.78 (C12,14), 128.24 (C11,15), 127.20 (C13), 114.96 (C5), 64.56 (C20), 55.33 (C19), 46.84 (C16), 43.93 (C9), 24.95 (C21), 22.38 (C17,18), 11.03 (C22).

**$L_5$ :** Yield: ~65%; Anal. Calc. for  $\text{C}_{17}\text{H}_{22}\text{N}_6\text{O}_1$ : C, 62.5; H, 6.8; N, 25.8. Found: C, 62.8; H, 6.7; N, 25.6%.  $^1\text{H NMR}$  (DMSO- $d_6$ , ppm): 7.77 (bs, 1H, (N6)H), 7.79 (s, 1H, (C8)H), 7.36 (d, 2H, (C11,15)H,  $J = 7.7$  Hz), 7.28 (tt, 2H, (C12,14)H,  $J_a = 7.3$  Hz,  $J_b = 2.2$  Hz), 7.19 (tt, 1H, (C13)H,  $J_a = 7.3$  Hz,  $J_b = 2.2$  Hz), 6.14 (t, 1H, (N2)H,  $J = 5.6$  Hz), 5.11 (s, 1H, (O1)H), 4.64 (t, 1H, (N6)H,  $J = 5.3$  Hz), 4.54 (sep, 1H, (C16)H,  $J = 6.8$  Hz), 3.51 (q, 2H, (C20)H,  $J = 6.0$  Hz), 3.32 (q, 2H, (C19)H,  $J = 6.0$  Hz), 1.46 (d, 6H, (C17,18)H,  $J = 6.8$  Hz).  $^1\text{H NMR}$  (MeOH- $d_3$ , ppm): 7.78 (s, 1H, (C8)H), 7.36 (dd, 2H, (C11,15)H,  $J_a = 7.7$  Hz,  $J_b = 1.7$  Hz), 7.29 (tt, 2H, (C12,14)H,  $J_a = 7.3$  Hz,  $J_b = 2.2$  Hz), 7.21 (tt, 1H, (C13)H,  $J_a = 7.3$  Hz,  $J_b = 2.2$  Hz), 4.74 (s, 2H, (C9)H), 4.64 (sep, 1H, (C16)H,  $J = 6.8$  Hz), 3.69 (t, 2H, (C20)H,  $J = 5.8$  Hz), 3.50 (t, 2H, (C19)H,  $J = 5.8$  Hz), 1.54 (d, 6H, (C17,18)H,  $J = 6.8$  Hz).  $^{13}\text{C NMR}$  (DMSO- $d_6$ , ppm): 159.00 (C2), 154.42 (C6), 150.72 (C4), 140.65 (C10), 134.95 (C8), 127.95 (C11,15), 126.33 (C13), 113.61 (C5), 60.32 (C20), 45.52 (C16), 43.62 (C19), 42.66 (C9), 21.96 (C17,18).

**$L_6$ :** Yield: 75%, Anal. Calc. for  $\text{C}_{19}\text{H}_{26}\text{N}_6\text{O}_3$ : C, 59.0, H, 6.8, N, 21.8. Found: C, 58.8, H, 6.8, N, 21.6%. TLC: one spot.  $^1\text{H NMR}$  (DMSO- $d_6$ ,

ppm): 9.00 (bs, 2H, (O2,3)H), 7.76 (s, 1H, (C8)H), 7.58 (bs, 1H, (N6)H), 6.20 (d, 2H, (C11,15)H,  $J = 2.2$  Hz), 6.04 (t, 1H, (C13)H,  $J = 2.2$  Hz), 5.79 (d, 1H, (N2)H,  $J = 8.2$  Hz), 4.54 (s, 1H, (O1)H), 4.54 (sep, 1H, (C16)H,  $J = 6.8$  Hz), 4.54 (s, 2H, (C9)H), 3.81 (m, 1H, (C19)H), 3.48 (m, 1H, (C20)H<sub>a</sub>), 3.39 (m, 1H, (C20)H<sub>b</sub>), 1.61 (sep, 1H, (C21)H<sub>a</sub>,  $J = 7.3$  Hz), 1.47 (dd, 6H, (C17,18)H,  $J_a = 6.8$  Hz,  $J_b = 2.0$  Hz), 1.46 (sep, 1H, (C21)H<sub>b</sub>,  $J = 7.3$  Hz), 0.86 (t, 3H, (C22)H,  $J = 7.3$  Hz).  $^1\text{H NMR}$  (MeOH- $d_3$ , ppm): no visible (2H, (O2,3)H), 7.77 (s, 1H, (C8)H), 7.71 (bs, 1H, (N6)H), 6.31 (d, 2H, (C11,15)H,  $J = 2.2$  Hz), 6.14 (t, 1H, (C13)H,  $J = 2.2$  Hz), no visible (1H, (N2)H), no visible (1H, (O1)H), 4.61 (sep, 1H, (C16)H,  $J = 6.8$  Hz), 4.60 (s, 2H, (C9)H), 3.95 (m, 1H, (C19)H), 3.62 (m, 2H, (C20)H), 1.69 (sep, 1H, (C21)H<sub>a</sub>,  $J = 7.3$  Hz), 1.55 (dd, 6H, (C17,18)H,  $J_a = 6.8$  Hz,  $J_b = 1.5$  Hz), 1.54 (sep, 1H, (C21)H<sub>b</sub>,  $J = 7.3$  Hz), 0.97 (t, 3H, (C22)H,  $J = 7.3$  Hz).  $^{13}\text{C NMR}$  (DMSO- $d_6$ , ppm): 159.50 (C2), 158.64 (C12,14), 155.03 (C6), 151.19 (C4), 143.29 (C10), 135.38 (C8), 114.10 (C5), 105.47 (C11,15), 101.14 (C13), 63.53 (C20), 54.53 (C19), 46.15 (C16), 43.07 (C9), 24.36 (C21), 22.56 (C17), 22.47 (C18), 11.14 (C22).

### 3.3. Synthesis of $\text{Fe}(\text{III})$ complexes

A general pathway for the preparation of the complexes is as follows: totally 1 mmol of  $\text{FeCl}_3 \cdot \text{H}_2\text{O}$  (0.27 g) in ethanol (15 mL) was added to 1 mmol of  $L_n$  in ethanol (25 mL) and stirred (or kept in ultrasonic bath) at the temperature of 65 °C for approximately 3 h. After slow cooling, the reaction mixture was taken to vacuum desiccator to dry out. After few days, the orange-brown powder was washed by small amount of diethylether and dried again in desiccator with  $\text{P}_4\text{O}_{10}$  as a drying medium.

**1:** Yield: ~60%. Anal. Calc. for  $\text{C}_{18}\text{H}_{23}\text{N}_6\text{FeCl}_4$ : C, 41.6; N, 16.2; H, 4.4; Fe, 10.8. Found: C, 41.2; N, 16.0; H, 4.4; Fe, 10.6%. IR ( $\text{cm}^{-1}$ ): s = strong, m = medium, w = weak: 3400w, 3276w, 3105w, 2935w, 1638s (C=N), 1581m (C=C), 1535m, 1496m, 1452m (C=C), 1374m, 1351m, 1318w, 1280m, 1208m, 1179w, 1133m, 1080m, 1060m, 1027w, 884m, 763w, 753w, 699w, 658w, 640w, 602m, 484w. ES + MS ( $m/z$ ): 359 [ $L_1 + \text{H}$ ] $^+$ , 137 [adenine +  $\text{H}$ ] $^+$ .  $^1\text{H NMR}$  (DMF- $d_7$ , ppm): 9.48 (bs, 1H, (N6)H), 8.66 (bs, 1H, (C8)H), 7.53 (s, 2H, (C11,15)H), 7.37 (t, 2H, (C12,14)H,  $J = 7.2$  Hz), 7.30 (t, 1H, (C13)H,  $J = 7.3$  Hz), 5.38 (s, 1H, (N2)H), 4.90 (s, 2H, (C9)H), 4.80 (s, 1H, (C16)H), 3.80 (s, 2H, (C21)H), 3.62 (qui, 2H, (C19)H,  $J = 6.6$  Hz), 2.11 (s, 2H, (C20)H), 1.62 (s, 6H, (C17,18)H).  $^{13}\text{C NMR}$  (DMF- $d_7$ , ppm): 159.78 (C2), 155.18 (C6), 151.08 (C4), 143.24 (C8), 139.64 (C10), 129.54 (C12,14), 127.96 (C11,15), 128.58 (C13), 107.56 (C5), 59.38 (C20), 44.42 (C16), 42.42 (C19), 40.34 (C9), 20.21 (C17,18).

**2:** Yield: 45%. Anal. Calc. for  $\text{C}_{20}\text{H}_{30}\text{N}_6\text{O}_3\text{FeCl}_3$ : C, 42.6; N, 14.9; H, 5.3; Fe, 9.9. Found: C, 42.6; N, 14.6; H, 5.6; Fe, 10.1%. IR ( $\text{cm}^{-1}$ ): 3406w, 2968w, 2934w, 2877w, 1671s, 1635s (C=N), 1572 m (C=C), 1512m, 1461m (C=C), 1410m, 1373m, 1346w, 1316m, 1261m, 1214m (C<sub>ar</sub>-O), 1149m, 1120m, 1049m (C<sub>air</sub>-O), 925m, 886w, 819w, 769w, 717m, 642w, 558w. ES + MS ( $m/z$ ): 549 [ $\text{M} - (\text{H}_2\text{O}) + \text{H}$ ] $^+$ , 513 [ $\text{Fe}(\text{L}_2)\text{Cl}_2 + \text{H}$ ] $^+$ , 385 [ $\text{L}_2 + \text{H}$ ] $^+$ , 137 [adenine +  $\text{H}$ ] $^+$ .  $^1\text{H NMR}$  (DMSO- $d_6$ , ppm): 9.57 (bs, 1H, (O2)H), 8.17 (bs, 1H, (C8)H), 7.69 (bs, 1H, (N6)H), 6.99 (s, 1H, (C15)H), 6.90 (d, 1H, (C13)H,  $J = 8.1$  Hz), 6.72 (d, 1H, (C12)H,  $J = 8.1$  Hz), 5.11 (bs, 1H, (O1)H), 4.59 (sep, 1H, (C16)H,  $J = 6.8$  Hz), 4.56 (s, 2H, (C9)H), 3.84 (m, 1H, (C19)H), 3.61 (m, 2H, (C20)H), 2.16 (s, 3H, (C23)H), 1.62 (sep, 1H, (C21)H<sub>a</sub>,  $J = 7.3$  Hz), 1.54 (m, 1H, (C21)H<sub>b</sub>), 1.50 (dd, 6H, (C17,18)H,  $J_a = 6.8$  Hz,  $J_b = 1.8$  Hz), 0.87 (q, 3H, (C22)H,  $J = 7.3$  Hz).  $^1\text{H NMR}$  (MeOH- $d_3$ , ppm): 8.18 (s, 1H, (N6)H), 8.11 (s, 1H, (C8)H), 7.12 (s, 1H, (C15)H), 7.02 (d, 1H, (C13)H,  $J = 8.2$  Hz), 6.77 (d, 1H, (C12)H,  $J = 8.2$  Hz), 6.39 (s, 1H, (N2)H), 5.55 (s, 1H, (O1)H), 4.69 (s, 2H, (C9)H), 4.06 (m, 1H, (C19)H), 3.73 (s, 2H, (C20)H), 2.26 (s, 3H, (C23)H), 1.77 (sep, 1H, (C21)H<sub>a</sub>,  $J = 7.3$  Hz), 1.67 (m, 1H, (C21)H<sub>b</sub>), 1.62 (d, 6H, (C17,18)H,  $J = 6.8$  Hz), 1.04 (t, 3H, (C22)H,

$J = 7.3$  Hz).  $^1\text{H NMR}$  (acetone- $d_6$ , ppm): 8.47 (bs, 1H, (N6)H), 8.12 (bs, 1H, (C8)H), 7.16 (s, 1H, (C15)H), 6.96 (s, 1H, (C13)H), 6.78 (s, 1H, (C12)H), 6.47 (bs, 1H, (N2)H), 5.22 (bs, 1H, (O1)H), 4.80 (s, 2H, (C9)H), 4.68 (m, 1H, (C16)H), 4.09 (m, 1H, (C19)H), 3.76 (s, 2H, (C20)H), 2.21 (s, 3H, (C23)H), 1.81 (m, 1H, (C21)H<sub>a</sub>), 1.72 (m, 1H, (C21)H<sub>b</sub>), 1.65 (s, 6H, (C17,18)H), 1.03 (s, 3H, (C22)H).  $^1\text{H NMR}$  (DMF- $d_7$ , ppm): 9.88 (bs, 1H, (O2)H), 8.35 (s, 1H, (N6)H), 8.19 (bs, 1H, (C8)H), 7.16 (s, 1H, (C15)H), 6.96 (d, 1H, (C13)H),  $J = 8.1$  Hz), 6.80 (d, 1H, (C12)H),  $J = 8.1$  Hz), 5.90 (bs, 1H, (N2)H), 5.25 (bs, 1H, (O1)H), 4.72 (bs, 2H, (C9)H), 4.72 (m, 1H, (C16)H), 4.04 (m, 1H, (C19)H), 3.66 (m, 2H, (C20)H), 2.19 (s, 3H, (C23)H), 1.77 (sep, 1H, (C21)-H<sub>a</sub>,  $J = 7.3$  Hz), 1.62 (sep, 1H, (C21)H<sub>b</sub>,  $J = 7.3$  Hz), 1.58 (d, 6H, (C17,18)H,  $J = 6.8$  Hz), 0.96 (t, 3H, (C22)H,  $J = 7.3$  Hz).  $^{13}\text{C NMR}$  (DMSO- $d_6$ , ppm): 158.43 (C2), 156.70 (C6), 153.25 (C11), 152.01 (C4), 139.25 (C8), 129.47 (C14), 129.02 (C15), 127.52 (C13), 124.35 (C10), 115.43 (C12), 111.50 (C5), 62.69 (C20), 54.73 (C19), 47.53 (C16), 24.15 (C21), 22.27 (C17,18), 20.72 (C23), 10.91 (C22).

**3:** Yield: ~50%. Anal. Calc. for  $\text{C}_{19}\text{H}_{30}\text{N}_6\text{O}_4\text{Fe}_1\text{Cl}_3$ : C, 40.2; N, 14.8; H, 5.3; Fe, 9.9. Found: C, 40.5; N, 14.9; H, 5.4; Fe, 9.9%. IR ( $\text{cm}^{-1}$ ): 3278w, 3130w, 2968w, 2935w, 2877w, 1667s, 1637s (C=N), 1589s (C=C), 1572m, 1529m, 1482m, 1459m (C=C), 1373m, 1317m, 1282m, 1257m, 1215m (C<sub>ar</sub>-O), 1157m, 1135m, 1051m (C<sub>alif</sub>-O), 998m, 920w, 884m, 863w, 781m, 768m, 728m, 694w, 671m, 639w, 602w, 446w. ES + MS ( $m/z$ ): 568 [M+H]<sup>+</sup>, 461 [Fe(L<sub>3</sub>)Cl+H]<sup>+</sup>, 371 [L<sub>3</sub>+H]<sup>+</sup>, 137 [adenine+H]<sup>+</sup>.  $^1\text{H NMR}$  (DMSO- $d_6$ , ppm): 9.36 (bs, 1H, (O2)H), 8.20 (bs, 1H, (C8)H), 7.11 (t, 1H, (C14)H,  $J = 7.9$  Hz), 6.77 (m, 2H, (C13,15)H), 6.64 (d, 1H, (C11)H,  $J = 7.9$  Hz), 5.14 (bs, 1H, (O1)H), 4.63 (s, 2H, (C9)H), 4.60 (qui, 1H, (C16)H,  $J = 6.7$  Hz), 3.84 (s, 1H, (C19)H), 3.43 (m, 2H, (C20)H), 1.61 (m, 1H, (C21)H<sub>a</sub>), 1.49 (d, 6H, (C17,18)H,  $J = 6.7$  Hz), 1.43 (m, 1H, (C21)H<sub>b</sub>), 0.87 (m, 3H, (C22)H).  $^1\text{H NMR}$  (MeOH- $d_3$ , ppm): 8.15 (bs, 1H, (C8)H), 7.21 (t, 1H, (C14)H,  $J = 7.8$  Hz), 6.87 (m, 2H, (C13,15)H), 6.76 (d, 1H, (C11)H,  $J = 8.2$  Hz), 4.68 (s, 2H, (C9)H), 4.65 (m, 1H, (C16)H), 4.04 (m, 1H, (C19)H), 3.70 (m, 2H, (C20)H), 1.73 (m, 1H, (C21)H<sub>a</sub>), 1.66 (m, 1H, (C21)H<sub>b</sub>), 1.63 (d, 6H, (C17,18)H,  $J = 6.7$  Hz), 0.96 (t, 3H, (C22)H,  $J = 7.3$  Hz).

**4:** Yield: 70%. Anal. Calc. for  $\text{C}_{19}\text{H}_{30}\text{N}_6\text{O}_3\text{Fe}_1\text{Cl}_3$ : C, 41.4; N, 15.2; H, 5.4; Fe, 10.1. Found: C, 41.6; N, 15.3; H, 5.4; Fe, 9.8%. IR ( $\text{cm}^{-1}$ ): 3412w, 3274w, 3084w, 3030w, 2966w, 2932w, 2876w, 1671s, 1634s (C=N), 1571m (C=C), 1527m, 1494m, 1453m (C=C), 1373m, 1352m, 1316m, 1285m, 1253m, 1215w, 1133m, 1051m (C<sub>alif</sub>-O), 1028m, 967m, 885w, 842w, 769w, 746m, 698m, 671m, 638w, 599w, 485w. ES + MS ( $m/z$ ): 483 [Fe(L<sub>4</sub>)Cl<sub>2</sub>+H]<sup>+</sup>, 445 [Fe(L<sub>4</sub>)Cl+H]<sup>+</sup>, 355 [L<sub>4</sub>+H]<sup>+</sup>, 137 [adenine+H]<sup>+</sup>.  $^1\text{H NMR}$  (DMSO- $d_6$ , ppm): 9.34 (bs, 1H, (N6)H), 8.27 (bs, 1H, (C8)H), 7.38 (d, 2H, (C11,15)H,  $J = 7.0$  Hz), 7.34 (t, 2H, (C12,14)H,  $J = 7.3$  Hz), 7.26 (t, 1H, (C13)-H),  $J = 7.0$  Hz), 5.23 (bs, 1H, (N2)H), 4.72 (bs, 2H, (C9)H), 4.60 (qui, 1H, (C16)-H),  $J = 6.9$  Hz), 4.60 (bs, 1H, (O1)H), 3.85 (s, 1H, (C19)H), 1.62 (m, 1H, (C21)H<sub>a</sub>), 1.49 (d, 6H, (C17,18)H,  $J = 6.8$  Hz), 1.45 (m, 1H, (C21)H<sub>b</sub>), 0.86 (t, 3H, (C22)H,  $J = 7.2$  Hz).  $^1\text{H NMR}$  (MeOH- $d_3$ , ppm): 8.15 (bs, 1H, (C8)H), 8.04 (bs, 1H, (N6)H), 7.44 d, 2H, (C11,15)H,  $J = 7.2$  Hz), 7.41 (t, 2H, (C12,14)H,  $J = 7.5$  Hz), 7.34 (t, 1H, (C13)H,  $J = 7.2$  Hz), 4.78 (bs, 2H, (C9)H), 4.72 (s, 1H, (C16)H), 4.04 (m, 1H, (C19)H), 3.70 (d, 2H, (C20)H,  $J = 4.2$  Hz), 1.74 (m, 1H, (C21)H<sub>a</sub>), 1.67 (m, 1H, (C21)H<sub>b</sub>), 1.63 (d, 6H, (C17,18)H,  $J = 6.7$  Hz), 1.02 (t, 3H, (C22)H,  $J = 7.5$  Hz).  $^1\text{H NMR}$  (DMF- $d_7$ , ppm): 9.25 (bs, 1H, (N6)H), 8.30 (bs, 1H, C8-H), 7.51 (d, 2H, (C11,15)H,  $J = 7.2$  Hz), 7.37 (t, 2H, (C12,14)H,  $J = 7.5$  Hz), 7.30 (t, 1H, (C13)H,  $J = 7.0$  Hz), 5.35 (bs, 1H, (N2)H), 4.87 (s, 2H, (C9)H), 4.74 (qui, 1H, (C16)H,  $J = 6.9$  Hz), 4.03 (m, 1H, (C19)H), 3.79 (m, 1H, (C20)H<sub>a</sub>), 3.65 (m, 1H, (C20)H<sub>b</sub>), 1.75 (m, 1H, (C21)H<sub>a</sub>), 1.60 (d, 6H, (C17,18)H,  $J = 6.7$  Hz), 1.60 (m, 1H, (C21)H<sub>b</sub>), 0.95t, 3H, (C22)H,  $J = 7.3$  Hz).  $^{13}\text{C NMR}$  (DMF- $d_7$ , ppm): 159.12 (C2), 156.11 (C6), 153.61 (C4), 143.52 (C10), 139.35 (C8), 128.97 (C12,14), 128.18 (C11,15), 127.70 (C13), 108.70 (C5),

63.51 (C20), 55.30 (C19), 48.05 (C16), 44.60 (C9), 24.48 (C21), 22.36 (C17,18), 10.82 (C22).

**5:** Yield: ~40%. Anal. Calc. for  $\text{C}_{17}\text{H}_{26}\text{N}_6\text{O}_3\text{Fe}_1\text{Cl}_3$ : C, 39.0; N, 16.1; H, 5.0; Fe, 10.7. Found: C, 39.0; N, 15.7; H, 4.7; Fe, 10.6%. IR ( $\text{cm}^{-1}$ ): 3394w, 3124w, 2977w, 2934w, 2878w, 1635s (C=N), 1574s (C=C), 1526m, 1496m, 1453m (C=C), 1409m, 1373m, 1352m, 1316m, 1277m, 1213m, 1133m, 1060m (C<sub>alif</sub>-O), 1027m, 882w, 769w, 748m, 726m, 699m, 670w, 638w, 599w, 485w. ES + MS ( $m/z$ ): 525 [M+H]<sup>+</sup>, 454 [Fe(L<sub>5</sub>)Cl<sub>2</sub>+H]<sup>+</sup>, 417 [Fe(L<sub>5</sub>)Cl+H]<sup>+</sup>, 327 [L<sub>5</sub>+H]<sup>+</sup>, 137 [adenine+H]<sup>+</sup>.  $^1\text{H NMR}$  (DMSO- $d_6$ , ppm): 8.77 (bs, 1H, (N6)H), 8.18 (bs, 1H, (C8)H), 7.38 (d, 2H, (C11,15)H,  $J = 7.7$  Hz), 7.32 (t, 2H, (C12,14)H,  $J = 7.3$  Hz), 7.25 (t, 1H, (C13)H,  $J = 7.3$  Hz), 6.79 (bs, 1H, (N2)H), 5.19 (bs, 1H, (O1)H), 4.67 (s, 1H, (N6)H), 4.61 (qui, 1H, (C16)H,  $J = 6.8$  Hz), 3.52 (m, 2H, (C20)H), 3.37 (m, 2H, (C19)H), 1.48 (d, 6H, (C17,18)H,  $J = 6.8$  Hz).  $^1\text{H NMR}$  (MeOH- $d_3$ , ppm): 8.18 (bs, 1H, (C8)H), 8.18 (bs, 1H, (N6)H), 7.44 (d, 2H, (C11,15)H,  $J = 7.7$  Hz), 7.41 (t, 2H, (C12,14)H,  $J = 7.3$  Hz), 7.34 (t, 1H, (C13)H,  $J = 7.3$  Hz), 4.75 (s, 2H, (C9)H), 4.63 (m, 1H, (C16)H), 3.75 (m, 2H, (C20)H), 3.60 (m, 2H, (C19)H), 1.61 (d, 6H, (C17,18)H,  $J = 6.8$  Hz).

**6:** Yield: 50%. Anal. Calc. for  $\text{C}_{19}\text{H}_{30}\text{N}_6\text{O}_5\text{Fe}_1\text{Cl}_3$ : C, 39.1; N, 14.4; H, 5.1; Fe, 9.6. Found: C, 39.2; N, 14.0; H, 5.4; Fe, 9.2%. IR ( $\text{cm}^{-1}$ ): 3412w, 3268w, 3121w, 2969w, 2935w, 2878w, 1638s (C=N), 1576m (C=C), 1521m, 1459m (C=C), 1373m, 1350m, 1285m, 1214m (C<sub>ar</sub>-O), 1161m, 1049m (C<sub>alif</sub>-O), 1013m, 998w, 887w, 843w, 767m, 637m, 600w, 519w. ES + MS ( $m/z$ ): 568 [(M-(H<sub>2</sub>O))+H]<sup>+</sup>, 477 [Fe(L<sub>6</sub>)Cl+H]<sup>+</sup>, 387 [L<sub>6</sub>+H]<sup>+</sup>, 137 [adenine+H]<sup>+</sup>.  $^1\text{H NMR}$  (DMSO- $d_6$ , ppm): 9.15 (bs, 2H, (O2,3)H), 8.13 (bs, 1H, (C8)H), 7.70 (bs, 1H, (N6)H), 6.19 (d, 2H, (C11,15)H,  $J = 1.5$  Hz), 6.08 (s, 1H, (C13)H), 5.01 (bs, 1H, (O1)H), 4.59 (sep, 1H, (C16)H,  $J = 6.8$  Hz), 4.50 (s, 2H, (C9)H), 3.83 (bs, 1H, (C19)H), 3.61 (m, 1H, (C20)H<sub>a</sub>), 3.52 (m, 1H, (C20)H<sub>b</sub>), 1.61 (m, 1H, (C21)H<sub>a</sub>), 1.53 (m, 1H, (C21)H<sub>b</sub>), 1.50 (d, 6H, (C17,18)H,  $J = 6.8$  Hz), 0.87 (m, 3H, (C22)H).  $^1\text{H NMR}$  (MeOH- $d_3$ , ppm): 8.15 (bs, 1H, (C8)H), 6.34 (d, 2H, (C11,15)H,  $J = 2.2$  Hz), 6.25 (t, 1H, (C13)H,  $J = 2.2$  Hz), 4.66 (bs, 2H, (C9)H), 4.03 (m, 1H, (C19)H), 3.71 (m, 2H, (C20)H), 1.75 (sep, 1H, (C21)H<sub>a</sub>,  $J = 7.3$  Hz), 1.65 (m, 1H, (C21)H<sub>b</sub>), 1.63 (d, 6H, (C17,18)H,  $J = 6.8$  Hz), 0.98 (t, 3H, (C22)H,  $J = 7.3$  Hz).

### 3.4. General methods

Elemental analyses (CHN) were performed on a Flash EA 1112 analyzer (ThermoFinnigan) and the content of Fe was determined by chelatometric titration with sulphosalicylic acid as an indicator. Infrared spectra were obtained on a FT-IR Nexus 670 spectrometer (Thermo Nicolet) by means of polyethylene discs or the Nujol technique (in the region 1500–600  $\text{cm}^{-1}$ ) and the KBr technique (in the region 400–4000  $\text{cm}^{-1}$ ). The transmission  $^{57}\text{Fe}$  Mössbauer spectra were collected at 300 and 5 K using a Mössbauer spectrometer in constant acceleration mode with a  $^{57}\text{Co}$ (Rh) source and cryomagnetic system (Oxford Instruments). The isomer shift values were calibrated to metallic  $\alpha$ -iron.  $^1\text{H}$  and  $^{13}\text{C}$  NMR spectra of the ligands and complexes were measured on a Bruker 300 Avance spectrometer with an inverse probe tuned at 300.13 MHz for  $^1\text{H}$  (concentrations ~0.5  $\text{mg mL}^{-1}$ ) and probe tuned at 75.47 MHz for  $^{13}\text{C}$  (concentrations ~10  $\text{mg mL}^{-1}$ ). Tetramethylsilane (TMS) was used as an internal reference standard during  $^1\text{H}$  and  $^{13}\text{C}$  NMR experiments. Conductivity measurements were made with a Cond340i/SET Conductivity Meter (WTW, Germany) in methanol and acetone solutions, at 25 °C. The concentration of the complexes in the solutions was  $10^{-3}$  M [22]. The magnetic susceptibility measurements were performed for all the compounds by the Faraday method at 298 K with  $\text{Hg}[\text{Co}(\text{SCN})_4]$  as a calibrant. In case of **1** and **4**, the temperature dependence of the magnetic susceptibility was measured over the interval of 298–80 K. The calculated molar susceptibilities were corrected for diamagnetism using Pascal constants [25]. The

positive ion electrospray (ES+) mass spectra were recorded using a flow injection mode on the Waters ZMD 2000 mass spectrometer with the mass-monitoring interval 40–1300 *m/z*. The spectra were collected using 3.0 s cyclical scans and applying the sample cone voltage 20 or 40 V and capillary voltage +3.0 kV, at the source block temperature 100 °C, desolvation temperature 250 °C, cone gas flow rate 50 L h<sup>-1</sup> and desolvation gas flow rate 500 L h<sup>-1</sup>. The mass spectrometer was directly coupled to a MassLynx data system. Thermogravimetric analysis (TGA) and differential scanning calorimetry (DSC) were both performed with XP-10 Thermogravimetric Analyzer (THASS, GmbH) in temperature range of 20–1000 °C (TGA) and 20–400 °C (DSC) with the temperature gradient of 5 °C min<sup>-1</sup>. All measurements were carried out in the air atmosphere.

### 3.5. X-ray crystallography

X-ray data of 2-chloro-6-benzylamino-9-isopropylpurine, **L**, i.e. an intermediate for the preparation of **L**<sub>1</sub>, **L**<sub>4</sub> and **L**<sub>5</sub>, were collected on a four-circle *k*-axis diffractometer Xcalibur2 (Oxford Diffraction Ltd.) equipped with the Sapphire2 CCD detector at 120 K. The Crysalis software package [32] was used for data collection and reduction. The structure was solved using direct methods (SHELX, Sheldrick 2008) [33] and refined anisotropically on *F*<sup>2</sup> using full-matrix least-squares procedure (SHELX, Sheldrick 2008) [33] with weight scheme  $w = 1/[\sigma^2(F_o^2) + (0.076P)^2 + 0.208P]$ , where  $P = (F_o^2 + 2F_c^2)/3$ . All hydrogen atoms of **L** were located from difference Fourier maps and their parameters were refined using the riding model with C–H distances of 0.95 and 0.99 Å and N–H distances of 0.88 Å, and with  $U_{iso}(H) = 1.2U_{eq}(CH, CH_2 \text{ and } NH)$  or  $1.5U_{eq}(CH_3)$ . Crystal data and structure refinement parameters for **L** are given Table 6.

### 3.6. Quantum chemical calculations

Theoretical calculations using the DFT (B3LYP) approach were used to verify the assumed structures of studied complexes. All calculations were performed using the Gaussian03 program [34]. Preliminary data were prepared on the HF/6–31\* level of theory. Then, geometries of the obtained structures were fully optimized at the B3LYP level. Wachter's original full-electron basis set [35] (contracted as 62111111/3311111/3111) with one set of polarization functions was used for the iron atom, while for all other atoms the 6-311G(d) basis set [36] was employed. Harmonic frequency analysis was used to verify the nature of founded stationary points as the minima as well as for the calculation of zero-point vibrational energies. Calculated infrared frequencies were not scaled. Mössbauer shifts  $\delta$  were calculated according to equation  $\delta = \alpha[\rho_0^A(0) - \rho_0^S(0)]$ , where  $\alpha$  a calibration constant ( $-0.395 \text{ mm s}^{-1} \text{ au}^3$ ) and non-relativistic electron density at the Fe nucleus of reference compound  $\rho_0^S$  ( $11614.10 \text{ au}^{-3}$ ) were obtained from previous calculations [37–39]. Electron densities  $\rho_0^A(0)$  at the <sup>57</sup>Fe nuclei of studied compounds were calculated with the AIM2000 program [40] that utilizes the wave functions generated by Gaussian03 program.

### 3.7. Biological activity testing

Human malignant melanoma cell line G-361, human osteogenic sarcoma cell line HOS, human chronic myelogenous leukaemia cell line K-562 and human breast adenocarcinoma cell line MCF-7 were used for a cytotoxicity determination of synthesized compounds by calcein acetoxymethyl (AM) assay, as it was described previously in the literature [15,26]. The tumour cells were maintained in plastic tissue culture flasks and grown on Dulbecco's modified Eagle's cell culture medium (DMEM) at 37 °C in 5% CO<sub>2</sub> atmosphere

**Table 6**

Crystal data and structure refinements for 2-chloro-6-benzylamino-9-isopropylpurine, **L**.

Empirical formula	C <sub>15</sub> H <sub>16</sub> ClN <sub>5</sub>
Formula weight	301.78
Temperature	100(2) K
Wavelength	0.71073 Å
Crystal system, space group	Triclinic, P-1
Unit cell dimensions	$a = 10.0218(2) \text{ \AA}$ , $\alpha = 77.189(2)^\circ$ $b = 11.9984(3) \text{ \AA}$ , $\beta = 69.640(2)^\circ$ $c = 13.4265(3) \text{ \AA}$ , $\gamma = 81.5677(19)^\circ$
Volume	1471.66(6) Å <sup>3</sup>
Z, Calculated density	4, 1.362 g cm <sup>-3</sup>
Absorption coefficient	0.261 mm <sup>-1</sup>
<i>F</i> (0 0 0)	632
Crystal size	0.25 × 0.25 × 0.20 mm
Theta range for data collection	2.61–25.00°
Limiting indices	–11 < <i>h</i> < 11, –13 < <i>k</i> < 12, –15 < <i>l</i> < 10
Reflections collected/unique	11643/4970 ( <i>R</i> (int) = 0.0250)
Max. and min. transmission	0.9497 and 0.9377
Refinement method	Full-matrix least-squares on <i>F</i> <sup>2</sup>
Data/restraints/parameters	4970/0/383
Goodness-of-fit on <i>F</i> <sup>2</sup>	1.027
Final <i>R</i> indices ( <i>I</i> > 2σ( <i>I</i> ))	<i>R</i> 1 = 0.0360, <i>wR</i> 2 = 0.1001
<i>R</i> indices (all data)	<i>R</i> 1 = 0.0554, <i>wR</i> 2 = 0.1117
Largest difference peak and hole	0.277 and –0.318 e Å <sup>-3</sup>

and 100% humidity. The cell suspension of approximate density  $1.25 \times 10^5$  cells mL<sup>-1</sup> was redistributed into 96-well microtitre plates (Nunc, Denmark). After 12 h of preincubation, the tested compounds (in the 0.5–50, 0.5–100, and 0.5–200 μM ranges) were added. Incubation lasted for 72 h. At the end of this period, the cells were incubated for 1 h with calcein AM and fluorescence of the live cells was measured at 485/538 nm (ex/em) with a Fluoroskan Ascent (Labsystems, Finland). IC<sub>50</sub> values, the drug concentration lethal to 50% of tumour cells, were estimated. The presented values are represented by arithmetic means determined from three values.

Human 6xHis-tagged cyclin E/Cdk2 complex was produced in Sf9 insect cells coinfecting with appropriate baculoviral constructs. The cells were harvested 70 h post infection in lysis buffer (50 mM Tris pH 7.4, 150 mM NaCl, 5 mM EDTA, 20 mM NaF, 1% Tween 20, protease inhibitors) for 30 min on ice and the soluble fraction was recovered by centrifugation at 14,000g for 10 min. The kinase was purified on NiNTA column (Qiagen) according to manufacturer's instructions. To carry out experiments on kinetics under linear conditions, the final point test system for kinase activity measurement was used. The assay mixture contained 1 mg/mL histone (Sigma Type III-S), 15 μM ATP, 0.2 μCi [ $\gamma$ -<sup>33</sup>P] ATP and tested compound in a final volume of 10 μL, all in reaction buffer: 50 mM Hepes pH 7.4, 10 mM MgCl<sub>2</sub>, 5 mM EGTA, 10 mM 2-glycerolphosphate, 1 mM NaF, 1 mM DTT and protease inhibitors; where Hepes = 4-(2-hydroxyethyl)piperazine-1-ethanesulfonic acid, EGTA = ethylene glycol-bis(2-aminoethylether)-*N,N,N',N'*-tetraacetic acid, and DTT = (dithiothreitol). After 10 min, the incubations were stopped by adding 5% H<sub>3</sub>PO<sub>4</sub> and spotted on P81 phosphocellulose paper (Whatman). After washing in 5% H<sub>3</sub>PO<sub>4</sub>, the kinase activity was measured by digital imaging analyzer BAS-1800 (Fuji-film). The kinase activity was expressed as a percentage of maximum activity, the IC<sub>50</sub> values were determined by graphic analysis.

### Acknowledgments

Authors thank the Ministry of Education, Youth and Sports of the Czech Republic (Grant nos. MSM6198959218, 1M6198959201) for financial support. Authors also thank to Assoc. Prof. Zdeněk Šindelář for the temperature dependence of magnetic

susceptibility measurements, and Mrs. Dita Parobková for her help with biological testing.

### Appendix A. Supplementary material

Additional crystallographic data are deposited as CCDC 738583 and can be obtained free of charge from the Cambridge Crystallographic Data Centre, 12 Union Road, Cambridge CB2 1EZ, UK; fax: (+44) 1223–336–033; email: deposit@ccdc.cam.ac.uk, or at <http://www.ccdc.cam.ac.uk>. Selected bond lengths and angles, as well as a view of the molecular structure of the **L** ligand are deposited. Supplementary data associated with this article can be found, in the online version, at doi:10.1016/j.jinorgbio.2009.12.002.

### References

- [1] P. Cohen, *Nat. Cell Biol.* 4 (2002) E127–E130.
- [2] D.O. Morgan, *Nat. Cell Biol.* 4 (2002) E127.
- [3] P. Cohen, *Nat. Rev. Drug Discov.* 1 (2002) 309–315.
- [4] C. Benson, S. Kaye, P. Workman, M. Garrett, M. Walton, J. de Bono, *Brit. J. Cancer* 92 (2005) 7–12.
- [5] P.M. Fischer, A. Gianella-Borradori, *Expert Opin. Invest. Drugs* 14 (2005) 457–477.
- [6] Y.T. Chang, N.S. Gray, G.R. Rosania, D.P. Sutherlin, S. Kwon, T.C. Norman, R. Sarohia, M. Leost, L. Meijer, P.G. Schultz, *Chem. Biol.* 6 (1999) 361–375.
- [7] L. Meijer, A. Borgne, O. Mulner, J.P.J. Chong, J.J. Blow, N. Inagaki, M. Inagaki, J.G. Delcros, J.P. Moulino, *Eur. J. Biochem.* 243 (1997) 527–536.
- [8] W.F. De Azevedo, S. Leclerc, L. Meijer, L. Havlíček, M. Strnad, S.H. Kim, *Eur. J. Biochem.* 243 (1997) 518–526.
- [9] S. Wittmann, P. Bali, S. Donapaty, R. Nimmanapalli, F. Guo, H. Yamaguchi, M. Huang, R. Jove, H.G. Wang, K. Bhalla, *Cancer Res.* 63 (2003) 93–99.
- [10] D.E. MacCallum, J. Melville, S. Frame, K. Watt, S. Anderson, A. Gianella-Borradori, D.P. Lane, S.R. Green, *Cancer Res.* 65 (2005) 5399–5407.
- [11] B. Shan, Y. Zhuo, D. Chin, C.A. Morris, G.F. Morris, J.A. Lasky, *J. Biol. Chem.* 280 (2005) 1103–1111.
- [12] L. Szűčová, Z. Trávníček, M. Zatloukal, I. Popa, *Bioorg. Med. Chem.* 14 (2006) 479–491.
- [13] Z. Trávníček, V. Kryštof, M. Šípl, *J. Inorg. Biochem.* 100 (2006) 214–225.
- [14] P. Štarha, Z. Trávníček, R. Herchel, I. Popa, P. Suchý, J. Vančo, *J. Inorg. Biochem.* 103 (2009) 432–440.
- [15] M. Maloň, Z. Trávníček, M. Maryško, R. Zbořil, M. Mašláň, J. Marek, K. Doležal, J. Rolčík, V. Kryštof, M. Strnad, *Inorg. Chim. Acta* 123 (2001) 119–129.
- [16] Z. Trávníček, J. Mikulík, M. Čajan, R. Zbořil, I. Popa, *Bioorg. Med. Chem.* 16 (2008) 8719–8728.
- [17] C.M. Mikulski, S. Cocco, N.D. Franco, T. Moore, *Inorg. Chim. Acta* 106 (1985) 89–95.
- [18] C.M. Mikulski, S. Cocco, N.D. Franco, N.M. Karayannis, *Inorg. Chim. Acta* 80 (1983) L23–L25.
- [19] A.N. Specca, C.M. Mikulski, F.J. Iaconianni, L.L. Pytlewski, N.M. Karayannis, *J. Inorg. Nucl. Chem.* 43 (1981) 2771–2779.
- [20] M.V. Capparelli, D.M.L. Goodgame, P.B. Hayman, A.C. Skapski, *Inorg. Chim. Acta* 125 (1986) L47–L49.
- [21] H.M. Schmalie, E. Gyr, E. Dubler, *Acta Crystallogr. C* 56 (2000) 957–959.
- [22] W.J. Geary, *Coord. Chem. Rev.* 7 (1971) 81–122.
- [23] F. Menil, *J. Phys. Chem. Solids* 46 (1985) 763–789.
- [24] I. Dézsi, P.J. Ouseph, P.M. Thomas, *J. Inorg. Nucl. Chem.* 36 (1974) 833–836.
- [25] O. Kahn, *Molecular Magnetism*, Wiley VCH Inc., New York, USA, 1993.
- [26] Z. Trávníček, M. Maloň, M. Biler, M. Hajdúch, P. Brož, K. Doležal, J. Holub, V. Kryštof, M. Strnad, *Transit. Met. Chem.* 25 (2000) 265–269.
- [27] C.J. Pouchert, *The Aldrich Library of Infrared Spectra*, third ed., Aldrich Chemical Co., Milwaukee, WI, USA, 1981.
- [28] G. Socrates, *Infrared and Raman Characteristic Group Frequencies (Tables and Charts)*, third ed., John Wiley & Sons Ltd., Chichester, England, 2001.
- [29] K. Nakamoto, *Infrared and Raman Spectra of Inorganic and Coordination Compounds*, fifth ed., John Wiley & Sons Ltd., New York, USA, 1997.
- [30] K. Brandenburg, *DIAMOND*, Release 3.2, Crystal Impact GbR, Bonn, Germany, 2009.
- [31] S. Wang, S.J. McClue, J.R. Ferguson, J.D. Hull, S. Stokes, S. Parsons, R. Weswood, P.M. Fischer, *Tetrahedron: Asymmetry* 12 (2001) 2891–2894.
- [32] CrysAlis CCD and CrysAlis RED, Oxford Diffraction Ltd, Abingdon, Oxfordshire, England, 2002.
- [33] G.M. Sheldrick, *Acta Cryst. A* 46 (2008) 112–122.
- [34] M.J. Frisch, G.W. Trucks, H.B. Schlegel, G.E. Scuseria, M.A. Robb, J.R. Cheeseman, J.A. Montgomery Jr., T. Vreven, K.N. Kudin, J.C. Burant, J.M. Millam, S.S. Iyengar, J. Tomasi, V. Barone, B. Mennucci, M. Cossi, G. Scalmani, N. Rega, G.A. Petersson, H. Nakatsuji, M. Hada, M. Ehara, K. Toyota, R. Fukuda, J. Hasegawa, M. Ishida, T. Nakajima, Y. Honda, O. Kitao, H. Nakai, M. Klene, X. Li, J.E. Knox, H.P. Hratchian, J.B. Cross, V. Bakken, C. Adamo, J. Jaramillo, R. Gomperts, R.E. Stratmann, O. Yazyev, A.J. Austin, R. Cammi, C. Pomelli, J.W. Ochterski, P.Y. Ayala, K. Morokuma, G.A. Voth, P. Salvador, J.J. Dannenberg, V.G. Zakrzewski, S. Dapprich, A.D. Daniels, M.C. Strain, O. Farkas, D.K. Malick, A.D. Rabuck, K. Raghavachari, J.B. Foresman, J.V. Ortiz, Q. Cui, A.G. Baboul, S. Clifford, J. Cioslowski, B.B. Stefanov, G. Liu, A. Liashenko, P. Piskorz, I. Komaromi, R.L. Martin, D.J. Fox, T. Keith, M.A. Al-Laham, C.Y. Peng, A. Nanayakkara, M. Challacombe, P.M.W. Gill, B. Johnson, W. Chen, M.W. Wong, C. Gonzalez, J.A. Pople, *Gaussian 03*, Revision C.02, Gaussian, Inc., Wallingford, USA, 2004.
- [35] A.J.H. Wachters, *J. Chem. Phys.* 52 (1970) 1033–1036.
- [36] R. Krishnan, J.S. Binkley, R. Seeger, J.A. Pople, *J. Chem. Phys.* 72 (1980) 650–654.
- [37] E. Fluck, in: V.I. Goldanskii, R.H. Herber (Eds.), *Chemical Applications of Mössbauer Spectroscopy*, Academic Press Inc., New York, 1968, pp. 268–311.
- [38] P. Gütllich, J. Enslin, in: A.B.P. Lever, E.I. Salomon (Eds.), *Inorganic Electronic Structure and Spectroscopy*, vol. 1, John Wiley and Sons, New York, 1999, pp. 161–212.
- [39] V.N. Nemykin, R.G. Hadt, *Inorg. Chem.* 45 (2006) 8297–8307.
- [40] F. Biegler-Konig, J. Schonbohm, D. Bayles, *J. Comput. Chem.* 22 (2001) 545–559.